LRIG3 IS NECESSARY FOR PROPER CELLULAR CENSUS IN THE STEM CELL COMPARTMENT OF THE COLONIC EPITHELIUM IN HOMEOSTASIS AND REGENERATION

by

JANELLE MARIE STEVENSON

A DISSERTATION

Presented to the Department of Biology
and the Division of Graduate Studies of the University of Oregon
in partial fulfillment of the requirements
for the degree of
Doctor of Philosophy

June 2022

DISSERTATION APPROVAL PAGE

Student: Janelle Stevenson

Title: Lrig3 is Necessary for Proper Cellular Census in the Stem Cell Compartment of the Colonic Epithelium in Homeostasis and Regeneration

This dissertation has been accepted and approved in partial fulfillment of the requirements for the Doctor of Philosophy degree in the Department of Biology by:

Victoria Herman	Chairperson
Anne Zemper	Advisor
Karen Guillemin	Core Member
Kryn Stankunas	Core Member
Carrie McCurdy	Institutional Representative

and

Krista Chronister Vice Provost for Graduate Studies

Original approval signatures are on file with the University of Oregon Graduate School.

Degree awarded June 2022

DISSERTATION ABSTRACT

Janelle Stevenson

Doctor of Philosophy

Department of Biology

June 2022

Title: Lrig3 is Necessary for Proper Cellular Census in the Stem Cell Compartment of the Colonic Epithelium in Homeostasis and Regeneration

The cellular census of the colonic crypt is tightly regulated to provide a protective barrier from the external environment and actively renew every five-to-seven days. The crypt is formed into U-shaped invaginations that compartmentalize cell type and function through three primary regions: the stem cell compartment at the base, the transit-amplifying region in the middle, and the differentiated region at the luminal surface. This steady state of renewal requires consistent and stereotyped cell proliferation, migration, differentiation, anoikis and extrusion from the epithelium. Every year, in millions of genetically-susceptible Americans, this process goes awry, and the disruption of the epithelial barrier results in an inflammatory response to commensal microbes and pathogens, resulting in Inflammatory Bowel Disease (IBD). This inflammatory attack results in complete, localized destruction of the epithelial layer and this is repaired, over time, and restored to its original state. The etiology of IBD is not fully understood, studying the molecular mechanisms and gene expression that governs colonic cell self-renewal

and crypt and regeneration will likely aid in our understanding of the regenerative process that occurs in IBD patients. In this thesis I show how Lrig3, a transmembrane protein, governs homeostatic renewal and inflammation-induced regeneration. I describe for the first time that Lrig3 is expressed in colonic crypt epithelial cells, including the stem, progenitor, and differentiated cell types. Using a novel mouse model, I show that mice missing Lrig3 have an expansion of the stem cell compartment in colonic crypts, without any obvious impact to colonic function. However, when the mice are subjected to a chemically induced inflammatory state, they lack the ability to regenerate their colonic epithelium. This thesis contributes key information in our understanding of cellular census in the colonic crypt during epithelial renewal and identifies a protein necessary for colonic crypt regeneration.

This dissertation contains previously published and co-authored material.

CURRICULUM VITAE

NAME OF AUTHOR: Janelle Stevenson

GRADUATE AND UNDERGRADUATE SCHOOLS ATTENDED:

University of Oregon, Eugene
California State University, Sacramento

DEGREES AWARDED:

Doctor of Philosophy, Biology, 2022, University of Oregon
Master of Arts, Stem Cell Biology, 2016, California State University, Sacramento
Bachelor of Science, Cell and Molecular Biology, 2013, California State University, Sacramento

AREAS OF SPECIAL INTEREST:

Cell Biology
Molecular Biology
Stem Cell Biology
Physiology

PROFESSIONAL EXPERIENCE:

Teaching Assistant, Department of Biology University of Oregon, Eugene 2016-2022

Teaching Assistant, Department of Biology California State University, Sacramento CA 2014-2016

Graduate Researcher in Knoepfler Lab UC Davis, CA 2014-2015

Patient Coordinator, California IVF, Davis, CA 2013-2014

Intelligence Analyst, US Army/Reserves 2002-2019

Research Assistant, Stem Cell Partners, Sacramento, CA 2011-2012

GRANTS, AWARDS, AND HONORS:

NIH Training Grant (T32HD007348), University of Oregon, 2018 – 2020

Bridges to Stem Cell Research Professional Science, UC Davis and California State University, Sacramento 2014-2016

Summer Undergraduate Research Experience Award, California State University, Sacramento 2012

PUBLICATIONS:

Stevenson, J. G., Sayegh, R., Pedicino, N., Pellitier, N. A., Wheeler, T., Bechard, M. E., Huh, W. J., Coffey, R. J., & Zemper, A. E. (2022). Lrig3 restricts the size of the colon stem cell compartment. *American Journal of Physiology - Gastrointestinal and Liver Physiology*. (In Review)

ACKNOWLEDGMENTS

I would like to express my appreciation and gratitude to my mentor Dr. Annie Zemper for providing training, guidance, and compassion throughout the past 6 years. Your leadership and direction have allowed me the time and space to explore my scientific interests and I am proud of the scientist I have become working in your lab. I have had the opportunity to grow as a scientist, a person, and a mother in the Zemper Lab and am better for having our "Lab Family". I'd like to thank our amazing technicians Bree Mohr, Natalie Pelletier, and Nick Jahahn for always supporting me at the bench, reading drafts of papers, and listening to many practice talks. I am extremely appreciative for Dr. Tim Wheeler, for always being there to tackle every challenge and hurdle of graduate school together, for the many scientific discussions, and for being a great friend always available for a chat. Thank you to Rachel Hopton for always being there to listen to ideas about projects or general life disturbances. Thank you to Ryan Sayegh, Natalie Pedicino, and Kevin Meuller for working with me on my projects and being dedicated and hard-working undergraduate researchers.

I would also like to express my sincere gratitude to my committee – Dr. Tory Herman, Dr. Kryn Stankunas, Dr. Karen Guillemin, and Dr. Carrie McCurdy – for their invaluable insight into the formation of my project, continued guidance throughout graduate school, and genuine caring.

Finally, I would like to express my gratitude to my family. Thank you to my mom Cathy, for always believing in me and being just a phone call away at a moment's notice. Thank you to Mike, for always being there when we needed you and being the most amazing grandpa, we're lucky to have you in our lives. Thank you to Bradley, my younger brother, for being the first person in our family to pursue a graduate education and always encouraging my academic endeavors. Thank you to my in-laws Rhonda and Larry, who have always supported us and encouraged us to persevere.

But most of all thank you to my husband Evan and our children Evan Jr. and Evelyn. Thank you, Evan, for always supporting my dreams, being an amazing father to our children, and never letting me give up. Without your unwavering love and support, and willingness to become a stay-at-home dad during the pandemic, I would not be here today. Thank you to Evan and Evelyn for always being curious about science, being excited to join me in the lab on the weekends, and being the most amazing kids a mom could ask for! I love you and am excited to move into the next season of our lives as a family!

This work was supported in part by the Developmental Biology Training Grant, T32HD007348.

This dissertation is dedicated to
My husband Evan, and
Our children Evelyn and Evan Jr.
Thank you for being you!

TABLE OF CONTENTS

Chapter Page

LIST OF FIGURES

Figure Page

LIST OF TABLES

Table Page

CHAPTER I

INTRODUCTION TO THE RENEWAL AND REGENERATIVE CAPABILITIES OF THE COLONIC EPITHELIUM

Structure and Function of the Mammalian Colon

The mammalian adult colon is patterned and assembled to facilitate absorption of water and nutrients, secrete a double layer antimicrobial mucosal barrier, and serve as a protective interface between the external environment and internal body, while requiring sufficient and highly specific penetration for absorption of critical molecules. The colon is lined with simple columnar epithelial cells that display a broad heterogeneity of cell types, maintained through specific tissue patterning, cell polarity, and molecular signals. This single layer of epithelial cells comprise millions of colonic crypts, which are test tube-shaped invaginations, with a central luminal hole on the surface of the colon. The cellular "census," or populations of specific cell types that make up each crypt is facilitated by somatic stem cell renewal and a subsequent commitment to differentiation by daughter cells which leads to continuous renewal of this epithelial lining (Gehart & Clevers, 2019).

Colonic Crypt Renewal

The murine colon renews every 5-7 days initiated through asymmetrical stem cell divisions in the base of the crypt (Barker, 2013). The colonic crypt maintains a precise and tightly regulated stereotypic structure comprised of three cellularly and functionally specific regions (Fig 1). At the base of the crypt, resides the stem cell compartment, which consists of two primary cell types: somatic stem cells and differentiated secretory cells. The somatic stem cells, known as Crypt Base Columnar Cells (CBCs) and are identified by Leucine-rich repeat-containing G-protein coupled receptor 5 (*Lgr5*) expression. These stem cells are intercalated between differentiated secretory cells, known as Deep Crypt Secretory Cells (DCSs), which express a protein called Regenerating family member 4 (*Reg4*) (Sasaki et al., 2016). Stem cells in the colonic crypt are relatively fast cycling cells, where they divide asymmetrically approximately every 24-hours (Girish et al., 2021). This cell division produces one daughter cell identical to the original stem cell, which self-renews to preserve the stem cell population, and a second daughter cell is concurrently produced which will migrate upward to the Transit-Amplifying (TA) region. The stem cells receive signals from the neighboring support cells, as well as the mesenchymal cells residing immediately below the epithelial layer, to promote this carefully regulated process of renewal and asymmetric division (Fendrik et al., 2018).

The TA region resides in the middle of crypt, just above the stem cell compartment, and is comprised of the immediate daughter cells of the stem cells. These cells receive signals to commit to one of the two cell fate lineages that comprise the upper portion of the crypt, the secretory or absorptive lineage. The TA cells are highly proliferative, and express the cell cycle marker, Ki-67; it is in this compartment that the majority of the cellular expansion occurs, producing all of the differentiated cells that comprise the majority of the colonic epithelium (van der Flier & Clevers, 2009). Following proliferation and lineage commitment, the cells continue to migrate up the crypt to perform the necessary functions of the colon. The upper portion of the crypt is comprised of predominately differentiated secretory and absorptive cells, in a 1:3 ratio respectively, defined as goblet and colonocyte cells (Tóth et al., 2017). Finally, when the cells reach the luminal surface, or "colon cuff", they undergo a specialized form of programmed cell death

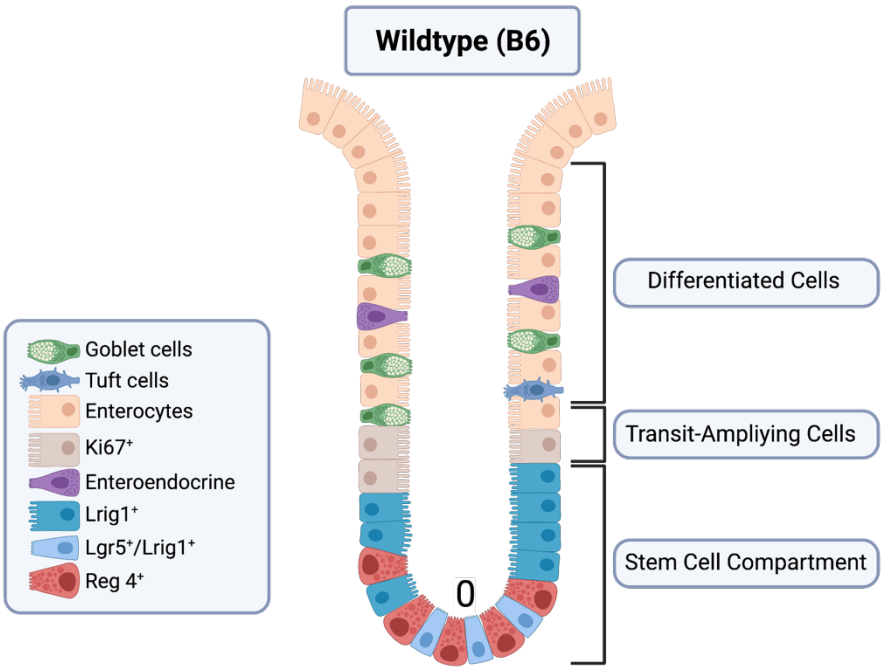

Figure 1. Graphical Representation of Colonic Crypt

called anoikis, are extruded into the lumen, and excreted (Ramachandran et al., 2000). This process allows for more space in the crypt to permit the continuous proliferation and migration, without the cells piling up on each other.

The Mouse as a Model for Colonic Crypt Renewal

The house mouse (*Mus musculus*) is a widely utilized model for investigations into the morphology, gene and protein expression, molecular mechanisms, and cell signaling, that regulate cellular renewal (Henning & von Furstenberg, 2016). The mouse colon is largely homologous to the human colon in structure and function, making it an ideal model to understand the molecular mechanisms of tissue self-renewal in higher-ordered organisms. Thousands of research articles are dedicated to understanding the composition of the cellular census of the colonic crypt in homeostasis and how this cellular composition directs the necessary form and function of the colon (Kwon et al., 2020; Tikhonova et al., 2020). Despite extensive research, it is still not fully understood what proteins and cell signaling pathways are required to develop and maintain the critical cellular stereotyping of the crypt. In Chapter 2, I explain how I use the mouse colon as a model system, and its stereotyped structure, to study a loss-of-function mutant; in this chapter, I will describe the discovery of protein responsible for the cellular census of the colonic stem cell compartment.

Colonic Regeneration in Response to Injury

Renewal of the colonic epithelium to produce the stereotyped regions of the colonic crypt have a specific function in maintaining a barrier to the luminal contents of the colon. In humans, there are a number of diseases that compromise this barrier, putting the human at risk for infection, inflammation and in some cases, cancer formation (Lucafò et al., 2021; Zhang & Li, 2014). There is a family of diseases that are involved in this barrier breach called Inflammatory Bowel Diseases (IBD) and they tend to arise suddenly, with no known cause (Xavier & Podolsky, 2007). During episodes of Inflammatory Bowel Disease (IBD) the colonic epithelial barrier function is reduced, localized infection from the commensal bacteria occurs and severe inflammation ensues, leading to destruction of the crypts in this inflamed area. These episodes typically resolve over the course of days or weeks, and this process involves the reduction of inflammation, and regeneration of the crypts (Yeshi et al., 2020). This proper regeneration of the colonic epithelium in and subsequent maintenance of the barrier from the external environment is critical for the survival of the organism.

The exact etiology of IBD is yet to be elucidated, however the generally accepted hypothesis is that IBD is an aggressive and inappropriate inflammatory response to an environmental trigger in people with a genetic predisposition to IBD (Park et al., 2020). There is a breadth of research investigating the etiology and underlying

mechanisms of IBD pathogenesis, and these have been invaluable for the development of clinical treatments for the symptoms of IBD. These therapeutics consist predominately of immunosuppressive drugs targeted at inhibiting inflammation, not the underlying cause of IBD, and therefore a great deal of investigation is still needed, focusing on molecular mechanisms initiated during an IBD inflammatory period. The lack of treatments targeted at the molecular mechanisms of regeneration in IBD, and other alternative therapies such as mucosal regeneration, is in part due a lack of understanding of the principal pathways involved (Villablanca et al., 2022). A deeper comprehension of the necessary proteins and critical signaling events will continue to advance therapies for patients and could potentially reduce the usage of chronic immunosuppressive drugs for IBD patients.

The mouse model is highly utilized to study IBD: the colonic regeneration, gene expression changes associated with regeneration, and signaling cascades following an inflammatory event (Kiesler et al., 2015). In Chapter 3, I utilize a mouse model to characterize protein expression following a chemically-induced inflammatory state that mimics human IBD. We then compare the results seen in the wildtype mice, to a mutant mouse model with a gene excised that is involved in cellular census of the colonic crypt stem cell compartment. Our IBD model allows us to investigate the protein expression, active signaling cascades, and

morphogenesis of the tissue at specific time points in the regenerative process – something that is currently impossible in humans.

In summary, during my doctoral work I discovered a protein necessary for establishing the cellular stereotyping and census of the colonic crypt in homeostasis and during regeneration. In chapter 2, I discuss how I established this mutant as an essential component of crypts and show these mutant murine colonic crypts harbor an expanded stem cell compartment. In Chapter 3, I demonstrate how these same mutant mice cannot regenerate their crypts after an IBD-like treatment. I intend for my doctoral work to add to the collection of knowledge regarding colonic crypt census and to add to the critically needed understanding in regeneration, to push the boundaries of innovation and allow for a widened variation of non-immunosuppressive therapies for patients living with IBD.

CHAPTER II

LRIG3 RESTRICTS THE SIZE OF THE COLON STEM CELL COMPARTMENT

*This chapter contains previously published co-authored material

Stevenson J.G., Sayegh R., Pedicino N., Pellitier N.A., Wheeler T., Bechard M.E., Huh W.J., Coffey R.J., Zemper A.E. Lrig3 restricts the size of the colon stem cell compartment. (In revisions, American Journal of Physiology – Gastrointestinal and Liver) Preprint
doi: https://doi.org/10.1101/2022.03.08.483523

Author contributions: All experiments in this chapter were performed, overseen and/or analyzed by me. Ryan Sayegh and Natalie Pedicino performed experiments and analyzed data. Natalie Pellitier and Tim Wheeler performed experiments. Matt and Won Jae provided valuable feedback and consultation regarding the manuscript and experimental protocols. Robert directed mouse genetics and provided valuable feedback on the manuscript. Annie and I conceived the project, designed experiments wrote and edited the manuscript. I created all the figures. Annie provided supervision, project administration, and funding.

Abstract

The cellular census of the colonic crypt is tightly regulated, yet the molecular mechanisms that regulate this census are not fully understood. Lrig3, a transmembrane protein, is expressed in colonic crypt epithelial cells, including the stem, progenitor, and differentiated cell types. Mice missing Lrig3 have a disruption in their cellular census: using a novel *Lrig3*$^{-/-}$ mouse we demonstrate that *Lrig3*$^{-/-}$ mice have more cells per crypt, a greater mucosal area, and longer colons compared to wildtype mice, suggesting the expression of Lrig3 is required for both the

total number of epithelial cells in the mouse colon, as well as colon length. In addition, we show *Lrig3*$^{-/-}$ mice have significantly more stem, progenitor, and deep crypt secretory cells, yet harbor a normal complement of enteroendocrine, Tuft, and absorptive cells. *Lrig3*$^{-/-}$ mice also have a concomitant decrease in phosphorylated Extracellular signal-related kinases, indicating the loss of Lrig3 leads to an expansion of the colonic stem cell compartment, in an Erk-dependent manner. Our study describes the expression of Lrig3 within the colon, defines perturbations in mice lacking *Lrig3,* and supports a role for Lrig3 in the establishment of both colonic crypt structure and cellular census, defined as the epithelial cell type and number in colon crypts.

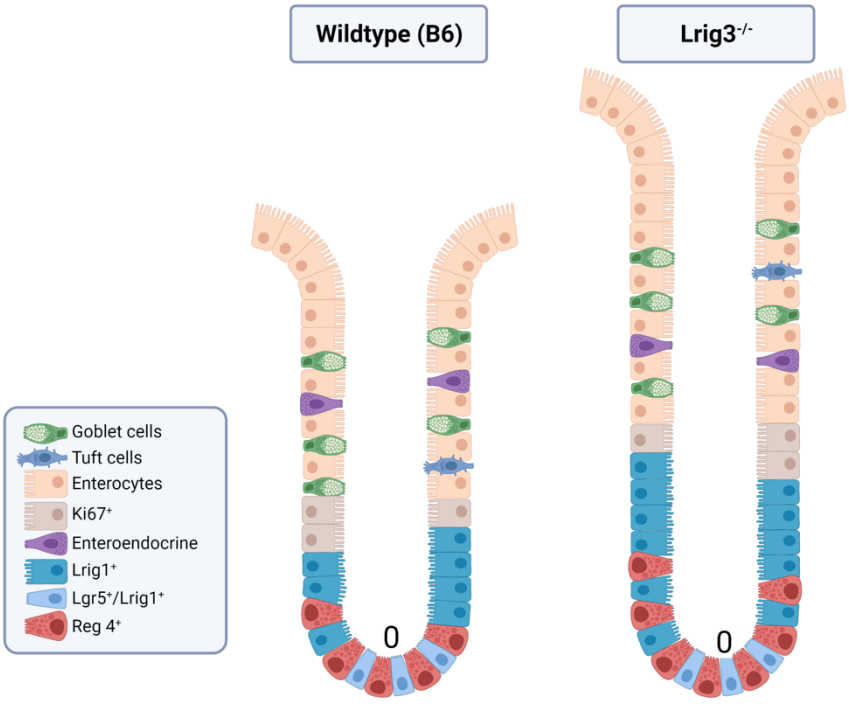

Figure 2. Graphical Abstract, model for expanded stem cell compartment in Lrig3$^{-/-}$

Introduction

Precise spatiotemporal regulation of stem cell proliferation, differentiation, and apoptosis are critical for proper regeneration of the gastrointestinal epithelium. In the mouse colonic epithelium, the majority of cells are renewed every five days driven by stem cell division at the base of the colonic crypt (Gehart & Clevers, 2019). In order to maintain crypt size and epithelial cell number, the cellular census is tightly regulated by balancing the number of stem, progenitor, and differentiated cells per crypt. We know that each of these cell types are key for the absorptive and secretory jobs of the colon (Kwon et al., 2020). Here, we evaluate how the loss of Leucine-rich repeats and immunoglobulin-like domains 3 (Lrig3) affects crypt cellular census and explore the impact of the loss of Lrig3 on these three critical cell types.

Lrig3 is a single-pass transmembrane protein and one of three members of the Lrig protein family (Simion et al., 2014). Lrig family members generally regulate both receptor tyrosine and serine/threonine kinases (Simion et al., 2014). To date, Lrig3 hasn't been as extensively studied as the other Lrig family members, yet we know it is expressed across endo-, meso- and ectodermal tissue types throughout embryonic development (del Rio et al., 2013). Disruptions in Lrig3 affect proper neural crest formation in Xenopus laevis and result in incomplete formation of the murine lateral semicircular canal (Abraira et al., 2008; Zhao et al., 2008). Generally, mice, sheep and pig are smaller if they have

a loss-of-function in Lrig3 (Abousoliman et al., 2021; Hellström et al., 2016; Metodiev et al., 2018). Only recently have contributions to primary literature uncovered mechanistic roles for Lrig3 in the progression of many cancer cell types: cervical, hepatocellular, prostate, glioblastoma and colon (Cai et al., 2009; Chen et al., 2019; Hu et al., 2021; C. Peng et al., 2021; H. Sun et al., 2021; S. Sun et al., 2020; Zeng et al., 2020a).

While most adult vertebrates can survive and maintain some sort of homeostasis with the loss of Lrig3, there are a number of defects that have been described in knockout mice, including cardiac hypertrophy, misregulation of insulin levels and the misorganization of neurons in the central nervous system (de Vincenti et al., 2021; Hellström et al., 2016). In certain tissues, Lrig3 works in concert with another family member, Lrig1 (de Vincenti et al., 2021; del Rio et al., 2013). In the gastrointestinal tract, Lrig1 is expressed on stem and progenitor cells in the small intestine and colon and is functionally important for maintaining homeostasis. The loss of Lrig1 results in aberrant growth factor signaling and tumor formation (Powell et al., 2012; Wang et al., 2015). From publicly available expression databases, we know Lrig3 is also highly expressed in the gastrointestinal tract (*Genepaint*, n.d.) and Lrig3 protein is predicted to have striking homology to Lrig1 (Simion et al., 2014). These reasons led us to hypothesize that Lrig3 is important for development and homeostasis of the mouse colon. The goal of our study was to understand the impact of the loss of Lrig3 on colon biology.

Through transcript and protein expression analysis, we show that Lrig3 is present throughout the colonic crypt epithelium, and we describe multiple colon morphological and cellular defects in *Lrig3*$^{-/-}$ mice. Our study describes the expression of Lrig3 within the colon, defines perturbations in mice lacking Lrig3, and supports a role for Lrig3 in the establishment of both colonic crypt structure and cellular census, defined as the epithelial cell type and number in colon crypts.

Results

Lrig3 expression in colonic crypts

Our first step was to define Lrig3 expression in the colonic crypts by assessing *Lrig3* transcript and Lrig3 protein expression via in situ hybridization, immunofluorescence, and western blot analysis, respectively. We generated an *Lrig3* knockout mouse (*Lrig3*$^{-/-}$, Fig. 3A and Appendix A Fig. S1) to both serve as a control for these analyses and to evaluate the impact of the loss of *Lrig3*.

Further, Lrig3 protein is expressed in the majority of epithelial cells; this was confirmed by immunofluorescence and western blot analyses. Lrig3 protein was absent in *Lrig3*$^{-/-}$ mice (Fig. 3F-J). These results define, for the first time, Lrig3 expression in the mouse colonic crypt.

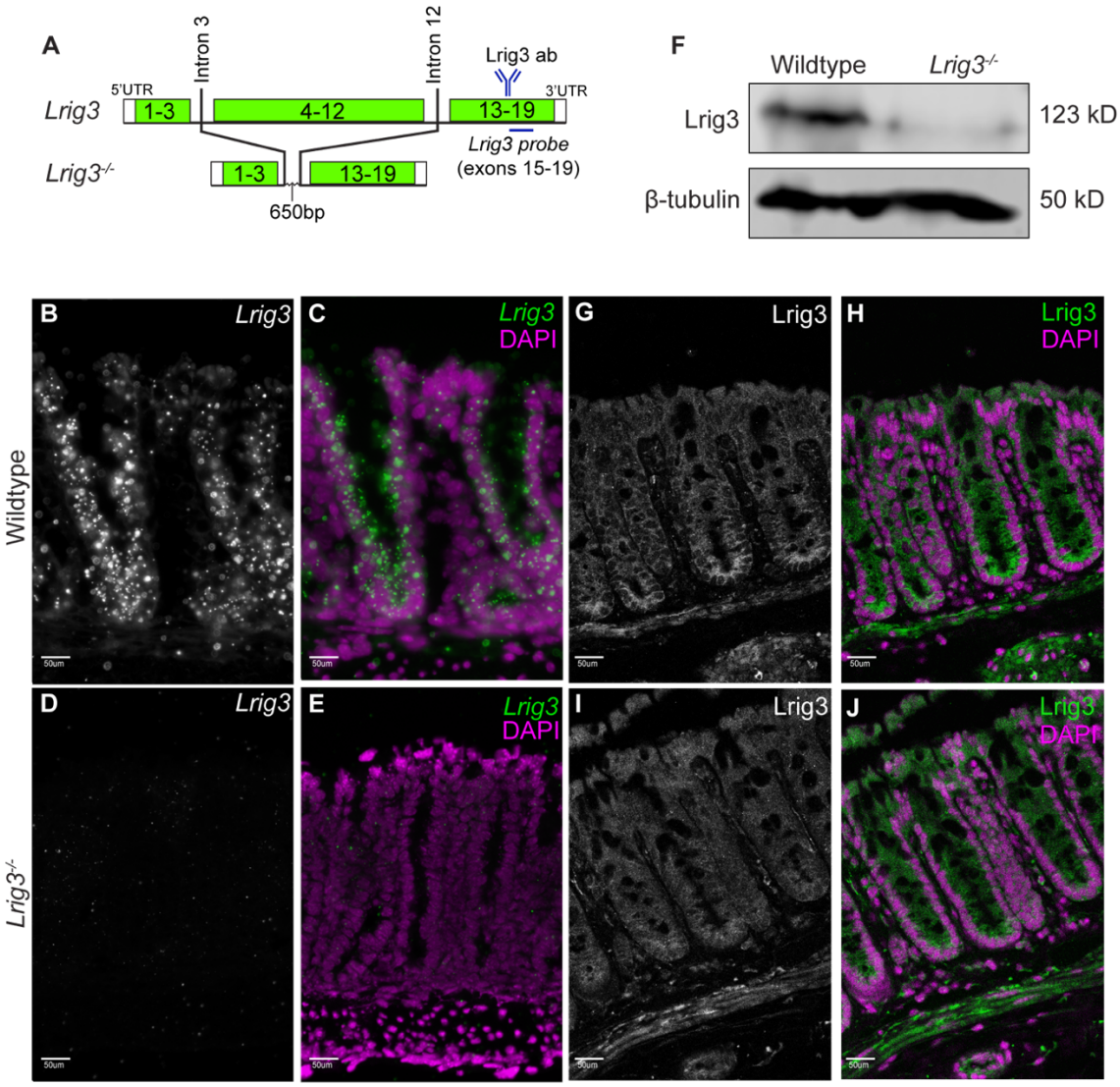

Figure 3. Lrig3 expression in the colonic epithelium.

A. Schematic depicting knockout of exons 4-12 in the *Lrig3*$^{-/-}$ mice, compared to WT mice. Blue antibody drawing indicates where Lrig3 antibody (panels F, G-J) antigen is located. Blue line indicates where *Lrig3* RNA SCOPE probe (panels B-E) is located. B-C. Representative epifluorescence RNA SCOPE images of colonic tissue cross sections indicating *Lrig3* transcripts (green) are located largely within the colonic epithelial compartment in wildtype mice. In *Lrig3*$^{-/-}$ mice (D-E), RNA SCOPE signal (green) is lost (n=3 mice/genotype, 16 images/mouse). F. Western blot comparing Lrig3 antibody reactivity in wildtype and *Lrig3*$^{-/-}$ colonic epithelial cell isolation lysates (n=3). G-J. Representative images from a single confocal slice illustrating Lrig3 antibody reactivity with wildtype (G-H) colonic tissue (green) cross-sections (n=3 mice/genotype, 10 images/mouse). Background fluorescence observed in *Lrig3*$^{-/-}$ (I-J). Scale bars indicate 50um. Nuclei in B-E and G-J are depicted in magenta. B, D, G and H are single channel representations of the green color shown in C, E, H and J, respectively.

Lrig3$^{-/-}$ mice have morphological and epithelial defects

As our initial results demonstrate that Lrig3 is highly expressed throughout the colonic crypt, we posited there may be epithelial disruption to the crypts in mice lacking Lrig3. Indeed, initial survey of the colonic tissues indicated morphological differences, as well as epithelial cellular census differences between WT and *Lrig3*$^{-/-}$ mice. To examine this directly, we first assessed colon lengths, and found that adult *Lrig3*$^{-/-}$ mice have significantly longer colons than WT mice at 6-10 weeks of age ($p<0.05$, Fig. 4A). We hypothesized that along with the observed increase in colon length there may be alterations at the cellular level. We examined this by measuring total mucosal area of WT and *Lrig3*$^{-/-}$ mice using hematoxylin and eosin stained, paraffin-embedded tissue sections and found that *Lrig3*$^{-/-}$ mice have a significantly larger mucosal area ($p<0.01$, Fig. 4B-D), per tissue section. The larger mucosal area in *Lrig3*$^{-/-}$ mice could be for several reasons, but we prioritized the investigation of two obvious hypotheses: 1) the epithelial cells within *Lrig3*$^{-/-}$ mice are larger or 2) there are more cells present in the crypts of *Lrig3*$^{-/-}$ mice. After an extensive examination of the colon sections from both sets of mice, we determined there was no obvious difference in cellular size between the cohorts (data not shown), ruling out that hypothesis. To investigate our second hypothesis, we quantified the number of epithelial nuclei per crypt, across both cohorts, and found that *Lrig3*$^{-/-}$ mice have more cells per colonic crypt than the WT mice ($p<0.05$, Fig. 4E). While there could be many reasons for a greater number of cells,

we first examined proliferation in the crypt of *Lrig3*$^{-/-}$ mice compared to WT mice by quantifying the expression of Ki67, a proliferative marker, in the epithelial cells. Surprisingly, we found no significant difference in the number of proliferating epithelial cells in the colonic crypts of *Lrig3*$^{-/-}$ mice at 6-10 weeks of age, compared to WT mice of the same age (Fig. 4F-J). From these analyses, we conclude that *Lrig3*$^{-/-}$ mice have a greater number of cells per crypt, but these cells are not undergoing aberrant proliferation.

Colon crypt stem cell compartments are expanded in *Lrig3*$^{-/-}$ mice

As epithelial cell number expansion is a hallmark of *Lrig3*$^{-/-}$ crypts, we wondered if this increased cell number was attributed to a particular region of the crypt. As there are many cell types present, we first assessed

---

Figure 4. Lrig3$^{-/-}$ mice have expanded mucosal area
A. Scatter plot indicating adult *Lrig3*$^{-/-}$ mice have significantly longer colons, as measured from cecum to rectum, compared to wildtype mice (n=10 mice/genotype). B. Scatter plot indicating adult *Lrig3*$^{-/-}$ mice have significantly more mucosal area in their colon, compared to wildtype mice (n=4, 10 images/mouse). C-D. Representative colon cross sections of wildtype and *Lrig3*$^{-/-}$ mice that have been stained with hematoxylin and eosin. Dashed line indicates the area measured for mucosal area. E. Scatter plot indicating adult *Lrig3*$^{-/-}$ mice have more nuclei per crypt compared to WT mice (n=4 mice/genotype, 10 images/mouse). F. Scatter plot indicating no significant change in proliferation (Ki67) between *Lrig3*$^{-/-}$ and wildtype mice (n=4 mice/genotype, 10 images/mouse, 152 crypts/genotype). G-J. Representative images of colonic tissue sections with anti-Ki67 antibody reactivity in *Lrig3*$^{-/-}$ (I-J) and wildtype (G-H) adult animals. Nuclei in H and J are depicted in magenta. In all plots, error bars indicate standard deviation from the mean. Significance was determined using an unpaired t-test where a significant difference between the groups is represented by an asterisk (*) when $p<0.05$. When $p<.01$., the data have been labeled with two asterisks (**), and by (****) when $p<0.0001$. Scale bar in C-D indicates 50um. All breaks in the Y axes are shown with parallel lines. G and I are single channel representations of the green color shown in H and J, respectively.

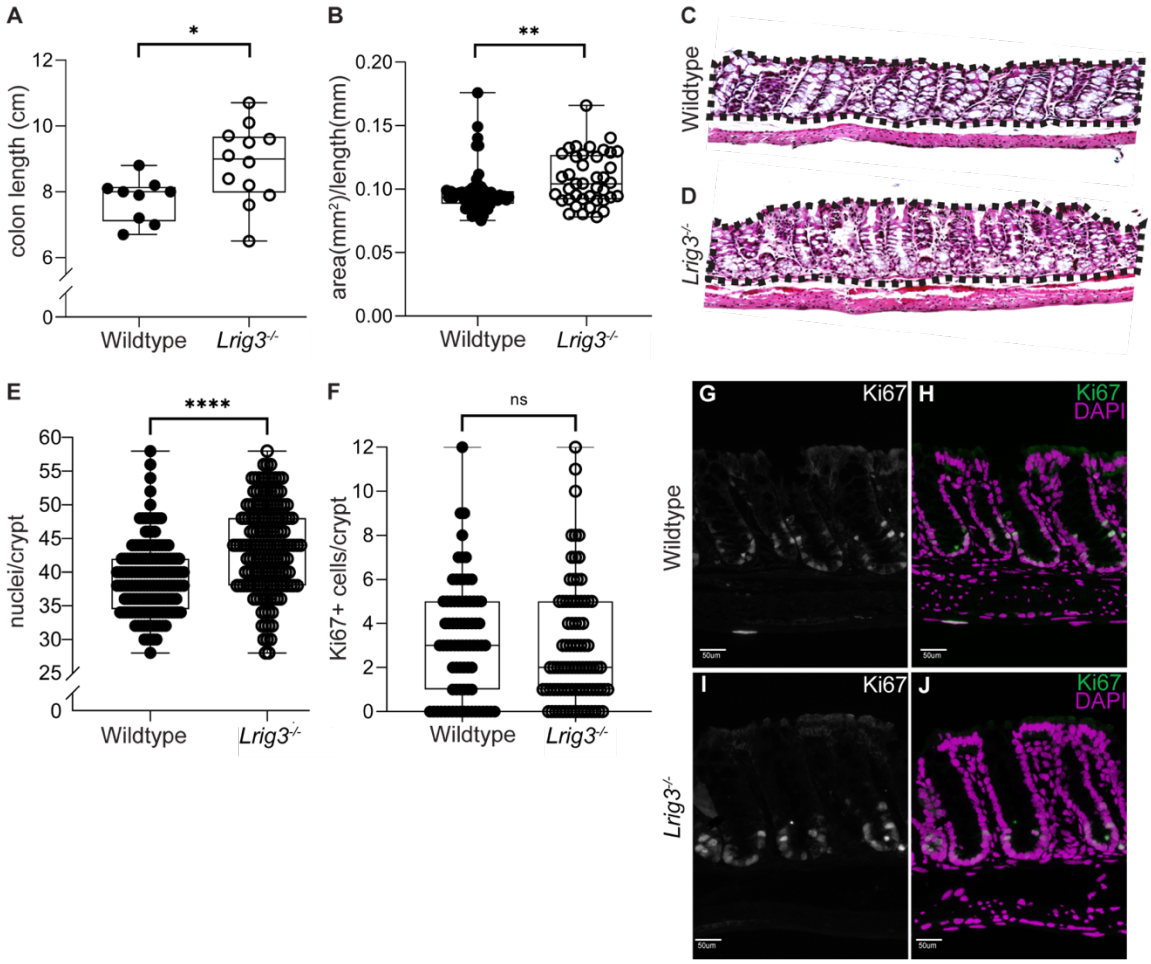

Figure 4.* Lrig3$^{-/-}$ *mice have expanded mucosal area

the stem and progenitor cells in the crypt-base by examining Lgr5 expression, as this is indicative of the presence of long-lived proliferative stem cells in the base of the colonic crypt (Barker et al., 2007). First, we performed RNA Scope in situ hybridization for Lgr5 expression and identified significantly more Lgr5+ cells in the colonic crypts of *Lrig3*$^{-/-}$ mice (Fig. 5A-D). In addition, some cells seemed to harbor qualitatively more Lgr5 than others, even in the WT tissue, consistent with previous analyses of stem and progenitor markers in the gut (Gehart & Clevers, 2019). To more carefully examine this observation, we devised a quantification scheme for looking at Lgr5 transcript expression levels in each cell. We binned them according to low- (<6 puncta per cell), mid- (6-14 puncta per cell), and high (15≤ puncta per cell) ranges (Fig. 5E). We quantified the puncta in *Lrig3*$^{-/-}$ and WT cells and while we observed no difference in the number of Lgr5 low-expressing cells, there were significantly more mid- and high-expressing cells in *Lrig3*$^{-/-}$ mice ($p<0.001$, Fig. 5F). The other cell type present in the stem cell region of the crypt is defined by the expression of the Reg4 protein. As Reg4+ cells act as support cells for Lgr5+ cells (Sasaki et al., 2016), we reasoned that we may also observe a parallel increase in Reg4+ cells, in *Lrig3*$^{-/-}$ mice. To determine this, we quantified the number of Reg4+ cells and found significantly more Reg4+ cells in the base of the crypt ($p<0.0001$, Fig. 5G-K). Reg4 is also expressed by secretory cells near the top of the crypt, thus we quantified the number of Reg4+ cells in

the upper half of the crypt and determined there is no change in the number of these cells between *Lrig3*$^{-/-}$ and WT mice (Fig. 5L). Finally, we examined the number of Vil-1+ (absorptive), Dclk1+ (Tuft), and ChgA+ (enteroendocrine) cells, which correspond to three additional differentiated cell types found in the upper portion of the crypts. Qualitatively, we found no obvious difference in Vil-1 expression, when comparing approximately 50 images per genotype. Quantitatively, we found no difference in Dclk1+ and ChgA+ cells when comparing *Lrig3*$^{-/-}$ and WT mice (Appendix B Fig. S2). Collectively, our results demonstrate the increased cell number we observe in *Lrig3*$^{-/-}$ mice is restricted to stem and support cells in the crypt base.

Figure 5. Expansion of the stem cell niche. A-D. Representative RNA SCOPE images of colonic tissue cross sections indicating *Lgr5* transcripts (green) between wildtype (A-B) and *Lrig3*$^{-/-}$ (C-D) mice. E. Representative images of low, mid, and high *Lgr5*+ transcript expression. F. Scatter plot indicating *Lrig3*$^{-/-}$ mice have significantly more *Lgr5*$^{+}$ mid and high cell transcript expression compared to wildtype mice (n=3 mice/genotype, 4 images/mouse). G-J. Representative images of colonic tissue sections comparing expression of Reg4 antibody reactivity. Dotted line depicts the center of the crypt where they were marked and quantified crypt upper half and lower half. K. Scatter plot indicating an increase in Reg4+ cells, in the lower half of the colonic crypt, in *Lrig3*$^{-/-}$ mice compared to wildtype mice (n=7 mice/genotype, 7 images/mouse). L. Scatter plot indicating no change in Reg4+ cells in the upper portion of the colonic crypt of *Lrig3*$^{-/-}$ mice compared to wildtype mice (n=7 mice/genotype, 7 images/mouse). Nuclei in B-E are depicted in magenta. Scale bar indicates 50um. In all plots, error bars indicate standard deviation from the mean. Significance was determined using an unpaired t-test where a significant difference between the groups is represented by an asterisk (*) when $p<0.05$. When $p<.01$., the data have been labeled with two asterisks (**), when $p<0.0001$, the data have been labeled with four asterisks (****). A, C, G and I are single channel representations of the green color shown in B, D, H and J, respectively.

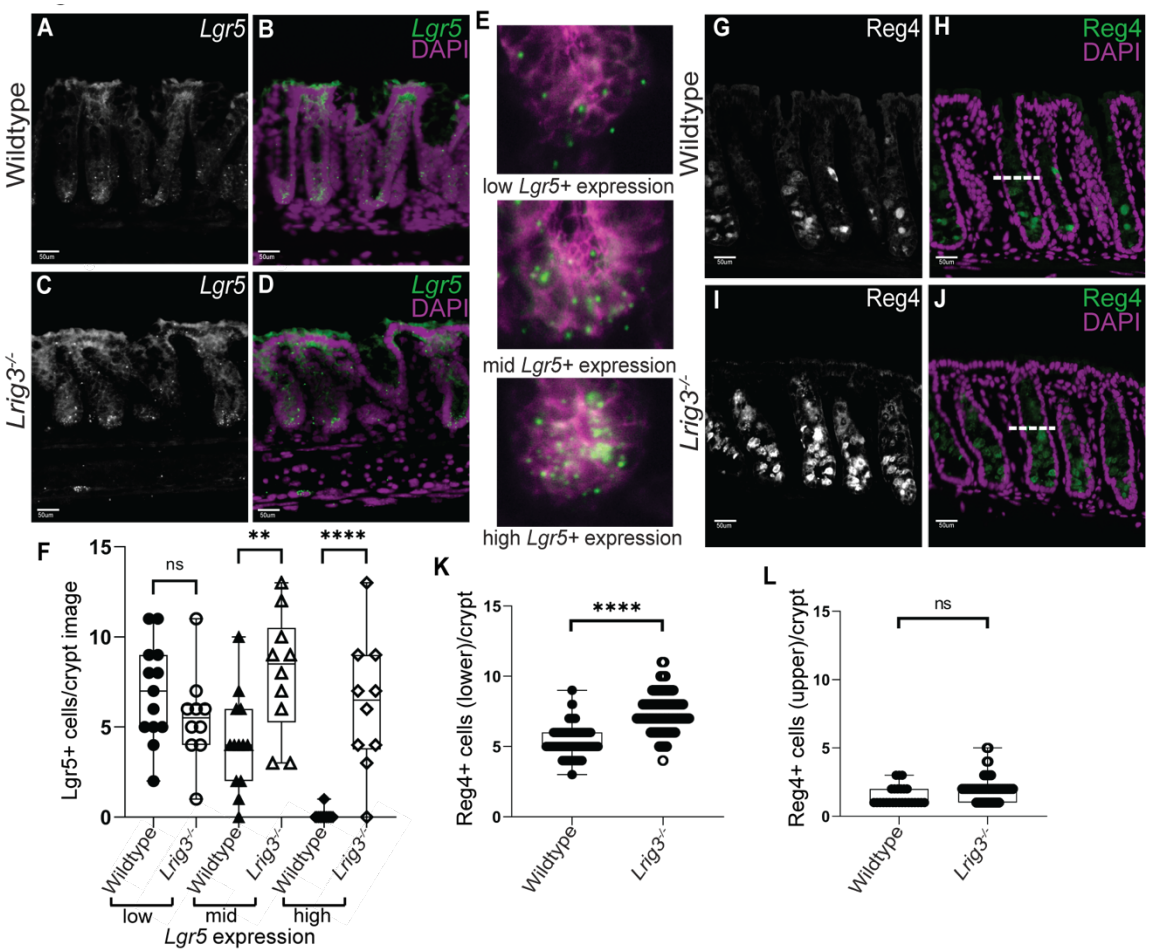

Figure 5. Expansion of the stem cell niche

Lrig3$^{-/-}$ mice have increased Lrig1 and decreased in pErk

As the stem cell niche is expanded in *Lrig3*$^{-/-}$ mice, we next examined if there was any change in expression of Lrig1, which is an Lrig3 family member, and widely expressed in intestinal stem and progenitor cells (Powell et al., 2012). While Lrig1 is normally restricted to the crypt-base, we found that *Lrig3*$^{-/-}$ mice have more Lrig1+ cells in the mid- and upper-crypt (Fig. 6A-D). We quantified the number of Lrig1+ cells per crypt and found significantly more Lrig1+ cells in *Lrig3*$^{-/-}$ mice compared to WT mice ($p<0.0001$, Fig. 6E). We also quantified Lrig1 expression in the crypts via western blot analysis and confirmed the increase in Lrig1 we detected in *Lrig3*$^{-/-}$ mice (Fig. 6F). As loss of Lrig1 results in changes to growth factor receptor signaling (Powell et al., 2012; Wong et al., 2012), we next assessed if the over-expression of Lrig1 seen in *Lrig3*$^{-/-}$ mice resulted in cell signaling changes in the crypts. We prioritized analysis of total and activated Epidermal growth factor receptor (Egfr and pEgfr, respectively), as these receptors are modulated based on Lrig1 expression (Powell et al., 2012). We also examined extracellular signal-related kinase (Erk) expression, as this is a transcriptional activator of proliferation and differentiation, and promoter of stemness in both the small intestine and colon (Osaki & Gama, 2013). We observed no obvious differences in the protein expression of total Egfr (Fig. 6G-H, K), activated Egfr or total Erk (Fig. 6I-K); however, we consistently observed decreased expression of phosphorylated Erk (pErk)

in the *Lrig3*$^{-/-}$ colonic crypts by western blot analysis (Fig. 6K). These results indicate this common downstream mediator of mitogen activated kinase signaling is changed in mice lacking Lrig3. Taken together, we observe that Lrig3 is required for proper Lrig1 expression and appropriate Erk activation.

Discussion

Using our novel *Lrig3*$^{-/-}$ mouse, we demonstrate that *Lrig3*$^{-/-}$ mice have more cells per crypt, a greater mucosal area, and longer colons compared to wildtype mice. This suggests the expression of Lrig3 is required for both the total number of epithelial cells in the mouse colon, as well as establishment of colon length. Further, we show *Lrig3*$^{-/-}$ mice have an Erk-associated expansion of the colonic stem cell compartment, as they harbor significantly more stem, progenitor, and deep crypt secretory cells.

Our research defines the expression domain of Lrig3, in the colon for the first time, as a novel marker of all colonic epithelial cells. The most well-studied Lrig family member, Lrig1 (Powell et al., 2012), is a homologue of Lrig3 with redundant expression patterns in some tissues (de Vincenti et al., 2021; del Rio et al., 2013). In the colon, Lrig1 expression is distinct from that of Lrig3, as it is restricted to the crypt-base (Powell et al., 2012; Wong et al., 2012). As their expression patterns are distinct in the gastrointestinal tract, it is likely that Lrig1 and Lrig3 also have unique molecular functions.

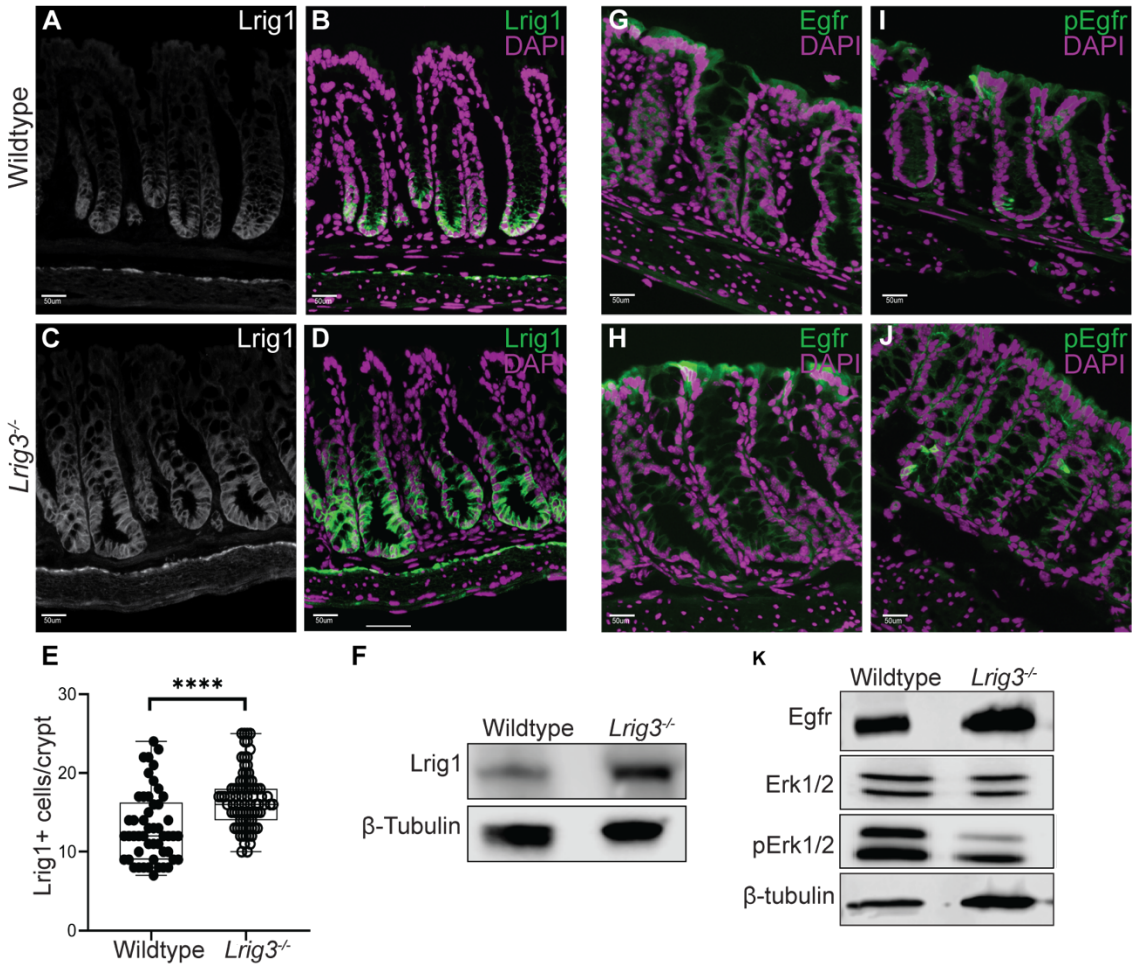

Figure *6*. Expression of Lrig1 is expanded in Lrig3$^{-/-}$ mice
A-D. Representative images of colonic tissue sections comparing the expression of Lrig1 between wildtype (A-B) and *Lrig3*$^{-/-}$ (C-D) mice. In A and C, Lrig1 (white) is detected at the cell membrane of cells located in the crypt base. In B and D, Lrig1 (green) is shown in the context of all cells in the crypt (magenta). E. Scatter plot indicating significantly more Lrig1^{+} cells in the colonic crypt of *Lrig3*$^{-/-}$ mice compared to wildtype (n=4 mice/genotype, 10 images/mouse). F. Western blot comparing Lrig1 antibody reactivity in wildtype and *Lrig3*$^{-/-}$ colonic tissue cell lysates (n=3). G-J. Representative images of colonic tissue sections comparing the expression of pEgfr (I and J, green) and Egfr (G-H, green) between wildtype and *Lrig3*$^{-/-}$ mice. K. Representative western blots comparing protein expression for Egfr, Erk1/2, and pErk1/2 in wildtype and *Lrig3*$^{-/-}$ colonic tissue cell lysates (n=3). Nuclei in G-J are depicted in magenta. Scale bars indicate 50um. Significance in scatter plot was determined using an unpaired t- test where a significant difference between the groups is represented by an asterisk (****) when $p<0.0001$. A and C are single channel representations of the green color shown in B and D respectively.

In vitro, we know that Lrig3 stabilizes the ErbB receptors, whereas Lrig1 promotes ErbB receptor degradation (Powell et al., 2012). It is less clear if Lrig3 also promotes stabilization of ErbB receptors in vivo; this observation may be tissue-dependent (Abraira et al., 2010). As with Lrig1, Lrig3 has been evaluated across many tissue types; and has a significant impact on growth factor receptor pathways. We show that one common mediator of ErbB and Ras signaling pathways, Erk, is dysregulated in *Lrig3*$^{-/-}$ mice. Through our examination of the ErbB family member, Egfr, we did not observe any changes to expression or activation of this powerful growth factor receptor in *Lrig3*$^{-/-}$ mice; the impact of Lrig3 loss on other growth cell signaling pathways represents an important area of future research. Lrig3 also has been shown to regulate fibroblast growth factor (FGF) receptors which results in changes to neural crest formation in frog (Zhao et al., 2008) and vascular endothelial growth factor (VEGF) receptors are modulated by Lrig3 in glioma (C. Peng et al., 2021; Zhou et al., 2021). Both FGF and VEGF pathways are important for the development and maintenance of the colonic epithelium (Dessimoz et al., 2006; Schlieve et al., 2016), but it is unknown if Lrig3 modulates these pathways in this context. This represents an important area of future research.

The question of how Lrig3 is regulated may be equally as important as the question as to what Lrig3 is regulating. Notably, Lrig3 expression is directly modulated by miRNA-196a, a microRNA that is upregulated in

gastric, colon, breast and pancreatic cancer and promotes tumorigenesis. In cervical cancer cells, miRNA-196a targets Lrig3 (Qiu et al., 2020) and improves cell viability. Lrig3 is also regulated at the post-transcriptional level, as there are reports of a circular form of Lrig3 (circRNA Lrig3) that is highly expressed in human hepatocellular carcinoma (HCC). Detection of blood plasma circ-Lrig3 is a highly sensitive and specific diagnostic indicator for HCC (H. Sun et al., 2021). Mechanistically, downregulation of circRNA Lrig3 represses both the MAPK/ERK and Smad pathways to prevent the progression of HCC and the loss of circRNA Lrig3 suppresses proliferation, invasion of HCC cells in vitro and blocks tumor growth of HCC in vivo (Hu et al., 2021; S. Sun et al., 2020). One recent report gives us a glimpse of the potential role in advanced colon cancer. Using human colon cancer cell lines, Zang and colleagues were able to show that Lrig3 represses metastasis-associated cell motility by inhibiting slug via inactivating ERK signaling (Zeng et al., 2020a). While the data on Lrig3 expression in solid tumors is expanding rapidly (Cai et al., 2009; Chen et al., 2019; Hu et al., 2021; C. Peng et al., 2021; H. Sun et al., 2021; S. Sun et al., 2020; Zeng et al., 2020a), the role of Lrig3 in the gastrointestinal tract at the genome, transcriptional and protein level is largely unknown and represents a valuable avenue for future research for both normal and cancerous colon tissue.

In terms of the requirement for Lrig3 in colon development and homeostasis, we have two key observations. The first is that *Lrig3*$^{-/-}$ mice

are born physically smaller and weigh less than their WT counterparts (Hellström et al., 2016), yet we also consistently observe these mice to have significantly longer colons at adulthood. While there has been a great deal of research defining the molecular requirements for small intestinal morphogenesis, and to some extent, for the colon (Dessimoz et al., 2006; Kwon et al., 2020), our results clearly signify the importance of studying Lrig3 and its role in colon development. While it is beyond the scope of this paper, a clear next step to understanding how Lrig3 impacts colon development is to take an in vivo, inducible loss-of-function approach for Lrig3, using a time course strategy to define the impact of loss of Lrig3 on birth weight and colon length.

Perhaps the most striking observation from our examination of *Lrig3*$^{-/-}$ mice is the greater number of cells per crypt despite no significant change to proliferation, resulting in *Lrig3*$^{-/-}$ mice having an expanded pool of stem and support cells in the crypt-base. While colonic epithelial self-renewal has been extensively researched (Gehart & Clevers, 2019) the majority of this research has been in adult mice, and generally has been assessed during regenerative phases after tissue injury (Yui et al., 2018). From these studies, we know the key signaling pathways that promote stem cell self-renewal and daughter cell differentiation (Gehart & Clevers, 2019). Cellular census (epithelial cell type and number) is generally consistent from crypt-to-crypt in the distal colon of both mice and humans. Unfortunately, there is a paucity of research examining the

molecular factors that regulate the number of colon cells and how the crypts arrive at a homeostatic census (and thus a consistent crypt size) in adulthood. Our data clearly demonstrate the requirement for proper Lrig3 expression to yield appropriate crypt cellular census. Despite the increase in cell number per crypt in *Lrig3*$^{-/-}$ mice, we do not observe an increase in all epithelial cell types. Indeed, we observe a specific increase in the number of cells in the stem cell compartment at the crypt-base, suggesting that Lrig3 is critical for establishing the size of the stem cell compartment during development. In future experiments, it will be important to test this hypothesis directly, either by overexpression of Lrig3 or through forced, wide-spread regeneration of colon crypts in *Lrig3*$^{-/-}$ mice. In the latter example, induction of acute injury to the adult *Lrig3*$^{-/-}$ colon to spur crypt renewal will be instructive in understanding how *Lrig3*$^{-/-}$ mice arrive at this aberrant state of homeostasis. Taken together, our results signify the importance of studying Lrig3 and its role in cellular census and colon development.

Experimental Procedures

Generating *Lrig3*$^{-/-}$ mice

The 129 Lrig3 BAC clone (bMQ-129G9) was obtained from Sanger Institute. The Lrig3 targeting construct which disrupts exons 4-12 of the Lrig3 locus was generated by BAC recombineering (Liu et al., 2003). The gene disruption strategy, null allele sequence and location of PCR primers is presented in Appendix Figure S1. PCR primer sequences are

listed in Table 1. ES cell electroporation and subsequent blastocyst injections were performed by the Transgenic Mouse/ES Cell Shared Resource at Vanderbilt University.

Table 1 WT and *Lrig3* Primers

WT and *Lrig3*$^{-/-}$ primers	
WT & *Lrig3*$^{-/-}$ 5' primer	5' gctaaagcagccacagagtggta 3'
WT 3' primer	5' ctgtgccctcaaactgtcaa 3'
Lrig3$^{-/-}$ 3' primer	5' ttccctggactggtaggtagctc 3'

Mice

C57BL/6 and *Lrig3*$^{-/-}$ mice were housed in a specific pathogen-free environment under controlled light cycle conditions, fed standard rodent lab chow, and provided water ad libitum. All procedures were approved and performed in accordance with the University of Oregon Institutional Animal Care and Use Committee. All mice were used at 6-10 weeks and mouse sex was mixed male to female at a roughly 50% ratio of each. All mice were sacrificed by cervical dislocation. At time of sacrifice, colons were removed, flushed with ice cold PBS and immediately measured using a ruler to obtain colon length, and then bifurcated.

Tissue Preparation for Staining

Tissue for paraffin and frozen block preparation were pinned onto a wax surface, fixed using 4% paraformaldehyde (PFA) for one hour (tissue imaged in Fig 3G-J were fixed in 4% PFA overnight), on a shaker at room temperature. They were then washed three times (five minutes each) in

PBS. For frozen blocks, tissue was submerged 30% sucrose in PBS overnight at 4°C and embedded in optimal tissue compound (OCT) for subsequent sectioning. For paraffin blocks, tissue was incubated in 70% ethanol and dehydrated in increasing alcohol baths and embedded in paraffin wax. All slides were sectioned at 7μm, (unless stated otherwise), and stained according to procedures below.

Colonic Crypt Protein Isolation

Bifurcated colons were cut into ~ 1cm pieces and incubated in ice cold 2mM EDTA and 0.5mM DTT PBS buffer, washed in PBS, and incubated 2mM EDTA buffer at 37°C. Tissue underwent vigorous lateral shaking to release crypts from submucosa, suspension was decanted, and shaking was repeated three times. The presence of single crypts is verified under a compound microscope and residual submucosal tissue is removed. The final collection of crypt suspensions was centrifuged at 500xg, cell pellet was then resuspended in Pierce RIPA buffer (ThermoFisher) with protease (½ tablet, Pierce Protease Inhibitor Mini tablets, EDTA-free, ThermoFisher) and phosphatase inhibitor (½ tablet PhosSTOP EASYpack, Roche), homogenized using an 18-gauge needle, and centrifuged at maximum speed. The supernatant was removed, and protein concentration determined using Pierce BCA kit (ThermoFisher).

Morphometric Analysis

Mucosal area and nuclei per crypt were quantified using paraffin embedded tissue and stained with Hematoxylin and Eosin (VWR). Images

and measurements were obtained on a Nikon Eclipse/Ds-Ri2. To quantify the mucosal area, we measured 10 images per animal (n=4 mice per genotype) using the Nikon NIS-Elements measurement tool. We measured the area of colonic epithelium by drawing lines across the basement membrane of the epithelium, along the sides, and across the luminal edge. To quantify the nuclei per crypt we used Hematoxylin and Eosin-stained paraffin slides and counted total nuclei per crypt in 10 images per animal (n=4 mice per genotype).

Antibodies and Staining Procedure

Frozen tissue slides were washed in PBS three times (three minutes each), blocked in 1% bovine serum albumin (BSA) and 0.03% Triton X-100 suspended in PBS for 1 hour. Antibodies were diluted in this blocking buffer at concentrations listed in Table 1, applied to the sections and sections were incubated overnight at 4°C. Slides were then washed in PBS three times (three minute each) and incubated with secondary antibodies at 1:500 in the same blocking buffer as above, for one hour at room temperature. Lastly, slides were washed in PBS for three minutes, then washed in PBS plus DAPI (1:10,000) for five minutes, and finally washed in PBS for three minutes. Slides were mounted using an n-propyl gallate/glycerol solution. Paraffin slides underwent conventional deparaffinization in xylenes and rehydration via ethanol washes and water, followed by antigen retrieval in a 1x Citrate buffer (ThermoFisher)

in a pressure cooker for one hour. Antibody catalog information and concentrations used are listed in Table 2.

Western Blot

Protein was diluted in a Laemmli buffer with 5% β-mercaptoethanol and boiled at 95°C for five minutes. 25μg of protein was loaded per lane into an SDS-PAGE gel (Bio-Rad Mini-Protean pre-cast gels 4-20%) and gels were run at 160V for approximately 90 minutes. Protein was transferred from the gel to a PVDF membrane overnight at 55V at 4°C. Membranes were blocked in either 5% dry milk or 5% BSA in PBS for one hour and incubated in primary antibody overnight at 4°C. Membranes are then incubated in HRP-conjugated secondary antibodies at room temperature for one hour. ECL reagent (GE Healthcare) was then applied, and subsequent images were captured on a LI-COR Odyssey Fc Imaging System. For quantification of protein levels of target proteins, β-tubulin was used as a normalization control (n=3 mice per genotype).

In Situ hybridization

In situ hybridization was conducted using RNAscope Multiplex Fluorescent Reagent Kit v2 (Advanced Cell Diagnostics #323110) according to manufacturer protocols for fixed, frozen tissue sample preparation protocol (ACD TN 320535 Rev A, 323100-USM). Briefly, 15um frozen sections were washed briefly in PBS, boiled for 5 minutes in 1x Target Retrieval buffer, followed by two brief washes in ddH_2O and one in 95% EtOH. Slides were dried then dammed with an ImmEdge

hydrophobic barrier pen, then incubated with Protease III for 15 minutes at 40°C. Slides were washed briefly in ddH_2O, then incubated at 40°C in sequence with Probe-Mm-Lgr5 (312171) or or Mm-Lrig3 probe (310541) (2hr), AMP 1 (30 min), AMP 2 (30 min), AMP 3 (15 min), HRP-C1 (15 min), Opal-570 TSA (30 min, 1:1000), with two two-minute washes with 1x Wash Buffer between hybridization steps. Slides were counterstained with DAPI and mounted with N-propyl gallate mounting medium.

Image acquisition and analysis

Images for quantification of all immunofluorescent and RNAscope images were obtained using a Nikon Eclipse/Ds-Ri2 and NIS Elements software tools. Lrig3 antibody was visualized using confocal microscopy on a Zeiss LSM-880 system. Images were false-colored in Adobe Photoshop. All image analysis and quantification was performed in a double-blind fashion and statistical comparisons were analyzed using GraphPad Prism software. Quantification of all images (total "n" and counting metrics) are designated in each figure legend, however there were two sets of images analyzed with different criteria and we explain them here. For the quantification of Lgr5 expression, images were acquired and binned according to low- (<6 puncta per cell), mid- (6-14 puncta per cell), and high (15< puncta per cell) expression levels. Example images are shown in Fig. 5E. For Reg4 quantification, we separated each colonic crypt in half (upper and lower regions) and counted the positive cells in each

region. Example images are shown in Fig. 5H and J, with the dotted white line separating upper from lower.

Table 2

Antibody	Company	Product#	Concentration
Lrig3	US Biological	151911	1:250(IF) 1:300 (WB)
Lrig1	R&D Systems	AF3688	1:500 (IF) 1:300 (WB)
Ki67(PE)	eBiosciences	SolA15	1:100 (IF)
Egfr	abcam	ab52894	1:500 (IF) 1:1000(WB)
pEgfr (Y1068)	abcam	200709	1:400 (IF)
Erk	Bioss	BS-0022R	1:1000 (WB)
pErk	Cell Signaling Technology	4370S	1:1000 (WB)
Reg4	R&D Systems	AF1379	1:100 (IF)

CHAPTER III

LRIG3 IS REQUIRED FOR COLONIC REGENERATION FOLLOWING DSS INDUCED COLITIS

^This chapter contains unpublished co-authored material.

Stevenson, Janelle; Mueller, Kevin; Bree Mohr, Natalie Pellitier, Zemper, Anne

Author contributions: I contributed to the conceptualization, methodology, data curation, analysis, figure creation, and wrote the chapter. Kevin Mueller performed experiments and analyzed data. Annie Zemper contributed to conceptualization, methodology, analysis, editing, supervision, project administration, and funding. Bree Mohr assisted in experiments. Natalie Pelletier assisted in experiments.

Introduction

Inflammatory Bowel Disease, primarily characterized as Ulcerative Colitis (UC) and Crohn's Disease (CD), was estimated to effect over 3 million Americans in 2015, a significant increase from 1.8 million in 1999 (Dahlhamer et al., 2016). People with IBD experience alternating periods of remission, with periods of "flare ups", or an active intestinal inflammatory state, throughout their lifetime. Periods of severe inflammation in CD and UC patients can significantly reduce quality of life and increases individual health care costs more than 3-fold (Park et al., 2020). As the incidence of IBD continues to increase in the US, and to become a greater disease burden worldwide, the etiology of the disease

is still not fully understood (Alatab et al., 2020). In general, it is widely accepted that IBD is an inappropriate and overly aggressive inflammatory response to microbes in a genetically susceptible host, with environmental factors triggering the onset or reactivation of an inflammatory disease state (Eichele & Kharbanda, 2017).

There is a deep breadth of research investigating the etiology and underlying mechanisms of IBD pathogenesis, that have been invaluable for the development of clinical treatments. However, current therapeutics consist predominately of immunosuppressive drugs targeted at inhibiting inflammation, not the underlying cause of IBD (Villablanca et al., 2022). Sustained investigation into the molecular mechanisms initiated during an IBD inflammatory period will continue to inform clinical therapies. The lack of treatments targeted at the molecular mechanisms of regeneration in IBD, and other alternative therapies such as mucosal regeneration, is in part due a lack of understanding of the principal pathways involved. A deeper comprehension of the necessary proteins and critical signaling events will continue to advance therapies for patients and could potentially reduce the usage of chronic immunosuppressive drugs for IBD patients.

Currently the murine (mouse) model is highly utilized to study regeneration and the associated gene expression and signaling cascades following an inflammatory event (Araki et al., 2010; B. Egger J. Lakshmanan, P. Moore, V. E. Eysselein, 2000; Chassaing et al., 2014;

Cochran et al., 2020; Eichele & Kharbanda, 2017). In fact, for more than 25 years, the mouse has provided an ideal model for understanding how the colon responds to inflammatory assaults, including both epithelial and immune responses (Kiesler et al., 2015).

There are three main modes of modeling colitis in mice: chemical, genetic and T-cell transfer. All cause inflammation and an epithelial regenerative response similar to that seen in IBD patients (Kiesler et al., 2015). Our lab uses a chemical model where acute inflammation of the colon is induced by the addition of Dextran Sodium Sulfate (DSS) to the drinking water of the mice. This induces an inflammatory state within the mid-to-distal colon, and when DSS is removed the inflammatory assault will subside and allow epithelial regeneration to occur. By initiating and stopping the chemical assault in the colon, cyclically, we can mimic the pathology of UC. DSS is a chemical agent with colitogenic and anticoagulant properties to induce epithelial damage and the most widely used experimental model to investigate the pathogenesis and etiology of human IBD (Eichele & Kharbanda, 2017).

Regeneration, following human UC flare ups and murine DSS induced inflammation, has been characterized by alternative mechanisms of cell signaling and gene expression than is seen in homeostatic regeneration. It is still not fully understood what proteins and cell signaling pathways are required to regenerate the critical cellular stereotyping of the crypt after inflammatory assault. Some posit that

residual progenitor cells left over after the assault has ended, expand to generate crypt-like structures. Others posit that differentiated cells "de-differentiate" to become more stem cell-like, to regenerate the epithelium. In either case, it has been established that the Lgr5+ population of cells responsible for normal crypt regeneration, are not present after DSS-induced colitis (Castillo-Azofeifa et al., 2019; Girish et al., 2021; Murata et al., 2020; Sasaki et al., 2016). Which cell or cells are responsible for salvaging the colonic epithelium after an inflammatory event remains an open area of research.

In the previous chapter, I characterized morphometric and molecular differences of the *Lrig3*$^{-/-}$ murine colonic epithelium compared to WT and identified an expansion of the stem cell compartment but no changes in the number of differentiated cells within the crypt. However, the changes identified have yet to recognize any functional deficiencies within the epithelium. Therefore, to better understand the regenerative capabilities of the colonic epithelium following an inflammatory state, I next wanted to investigate if the *Lrig3*$^{-/-}$ colonic epithelium can regenerate at the same capacity as the WT following an acute DSS-induced colitis.

Within this chapter provide the current status of this on-going project; I will discuss our experimental results alongside the relevance and future direction of the project. Ultimately, we found that loss of Lrig3 diminishes regeneration capacity in the colonic epithelium. Through morphological analysis, we show *Lrig3*$^{-/-}$ mice have increased

susceptibility to DSS-induced UC. Our study defines perturbations in the stem cell compartment after DSS-induced UC, in mice lacking Lrig3. Thus far, our study shows Lrig3 is required for colonic regeneration after DSS-induced UC, through the proper regulation of cell proliferation and death.

Results and Discussion

Morphometric Analysis

The first goal of our research was to test how *Lrig3*$^{-/-}$ mice respond to inflammatory challenge. In order to do this, we supplied WT and *Lrig3*$^{-/-}$ mice with 3% DSS in their drinking water for 6 days and allowed them to recover for 24 hours with untreated drinking water. Through weighing the mice daily, we found that *Lrig3*$^{-/-}$ mice lost a significantly higher percentage of their body weight than WT (Fig 7A, $p<0.001$). Upon dissection of the colons, we measured the colon length following a treatment cycle, as an additional metric to assess disease severity due to administration of DSS. Researchers have found that shortening of the colon following DSS treatment indicates increased susceptibility to the induced-inflammatory state (Chassaing et al., 2014). We found that following DSS treatment *Lrig3*$^{-/-}$ mice have significantly shorter colons WT mice (Fig 7B-C $p<0.0001$). In contrast, our previous study reported that *Lrig3*$^{-/-}$ mice have longer colons than WT mice at 6-10 weeks of age (Stevenson et al., 2022). The extreme shortening of the colon further emphasizes the susceptibility of *Lrig3*$^{-/-}$ mice to the inflammatory state.

Together, using the metrics of body weight lost and shortened colons allows us to determine the ability of the colonic epithelium to respond to the DSS treatment and recover through proper regenerative capability after the removal of DSS. The significant decrease in both body weight and colon length, due to DSS treatment, suggests that *Lrig3*$^{-/-}$ mice have a decreased ability to regenerate from an inflammatory state compared to WT mice.

In order to examine whether the colons of WT and *Lrig3*$^{-/-}$ mice were in a similar or differing regenerative state, we examined the number of cells per colon crypt. My first paper shows that *Lrig3*$^{-/-}$ mice have *more* cells per colonic crypt than WT mice at 6-10 weeks of age (Stevenson et al., 2022). So, we next quantified the number of nuclei per colonic crypt in DSS-treated mice. We found that following DSS treatment, *Lrig3*$^{-/-}$ mice have significantly fewer nuclei per crypt than WT mice (Fig 7D-E, $p<0.0001$). Following DSS treatment for 6 days and allowing 24 hours for recovery, both genotypes showed decreases in the average number of cells per crypt compared to homeostasis, however the *Lrig3*$^{-/-}$ mice lost a significantly more cells per crypt than WT mice. These results support the hypothesis that WT and *Lrig3*$^{-/-}$ mice are in a differing regenerative state after DSS and suggest that Lrig3 is required for protection against an inflammatory assault and/or epithelial regeneration following an inflammatory-like state.

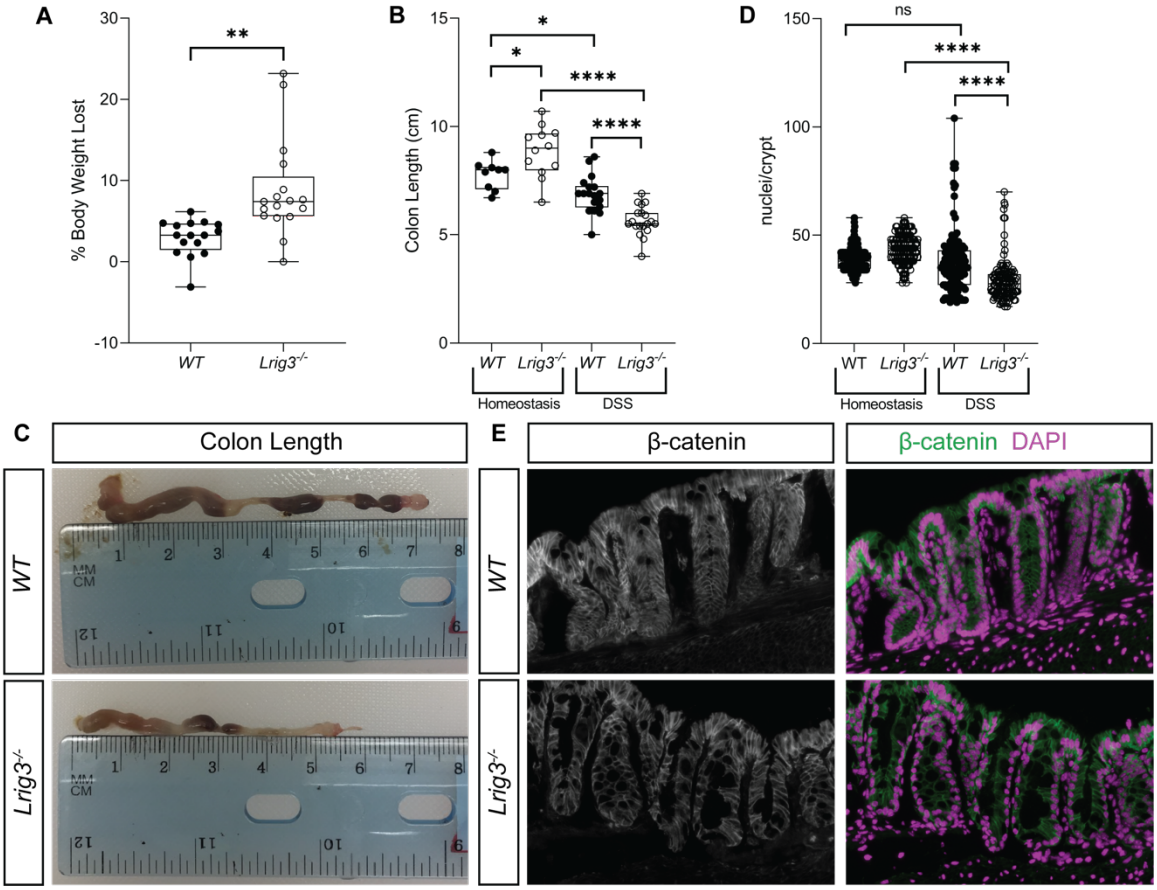

Figure 7. Morphological Defects in Lrig3$^{-/-}$ Mice Following DSS Treatment

A. Scatter plot indicating an increase in percentage of body weight lost 24 hours after DSS treatment in *Lrig3*$^{-/-}$ mice compared to *WT* mice (n=16 mice/genotype). B. Scatter plot indicating an increase in *Lrig3*$^{-/-}$ colon length in homeostasis compared to *WT* and a decrease in colon length 24 hours after DSS treatment compared to *WT* (n=9 homeostasis, n=18 DSS). C. Representative images of shortened colons after DSS. D. Scatter plot indicating more cells per crypt in *Lrig3*$^{-/-}$ mice in homeostasis and less cells per crypt in *Lrig3*$^{-/-}$ mice following DSS treatment, when compared to WT under same conditions. E. Representative image of DAPI and ß-catenin immunofluorescence used for nuclei quantification. Significance was determined using an unpaired t-test, where significant difference between the groups is represented by an (*) when $p<0.05$, (**) when $p<0.01$, and (****) when $p<0.0001$.

Proliferation and Cell Death

As total cell number in the crypt is ultimately governed by cell proliferation and/or cell death, we next wanted to examine the colonic epithelium of the DSS treated mice for nuclear markers of proliferation and death, to answer the question as to whether these cellular processes may be involved in the decreased regenerative capacity of *Lrig3*$^{-/-}$ mice. We hypothesized that the *Lrig3*$^{-/-}$ colonic epithelium has decreased proliferation and/or increased apoptosis compared to WT mice in the regenerative state, that is contributing to the change in cells per crypt that we identified.

To identify changes in proliferation, we conducted immunofluorescent staining for the proliferation marker, Ki67 (Brown & Gatter, 2002)and quantified the total number of Ki67+ cells per crypt on DSS treated WT and *Lrig3*$^{-/-}$ mice. We counted the number of Ki67+ cells per crypt and found significantly fewer proliferating cells *Lrig3*$^{-/-}$ crypts (Fig 8A-B) compared to the WT crypts. On average, DSS-treated *Lrig3-/-* mice contained an average of two Ki67+ cells per crypt and WT mice contained an average of six Ki67+ positive cells ($p=0.01$). In addition, it is important to note that *Lrig3*$^{-/-}$ mice have more cells per crypt in homeostasis, so this suggests that *Lrig3*$^{-/-}$ undergo a true inability to regenerate their epithelial population after a catastrophic event.

Our next step in cell analysis was to quantify the frequency of apoptosis occurring per crypt to determine if increased cell death in the *Lrig3*$^{-/-}$ crypts is contributing to decreased cells per crypt. To quantify cell death, we utilized an enzymatic TUNEL assay (J. Peng et al., 2020) to identify double stranded breaks in DNA and binned the data into three groups based on location of TUNEL signal within the crypt: lower half of the crypt, upper half of the crypt, and the cuff: luminal surface of crypts. Quantification of this data determined that there is increased apoptosis in both the lower ($p<0.005$) and upper ($p<0.01$) portions of the *Lrig3*$^{-/-}$ crypts, and no significant difference in the cuff (Fig 8C-D). Collectively, our cell death data show increased cell death in *Lrig3*$^{-/-}$ mice occurring within the colonic crypts, where we are less likely to visualize cellular apoptosis in WT mice, while apoptosis within the cuff, the region where cell death is expected to appear, is occurring on par with WT mice treated with DSS.

Figure 8. Cell proliferation decreases and cell death increases in Lrig3$^{-/-}$ mice following DSS A. Representative images of colonic tissue cross sections comparing expression of Ki67 protein (green) and DAPI (magenta) between *Lrig3*$^{-/-}$ and WT mice. B. Scatterplot indicating significantly less Ki67+ cells in the colonic crypt of *Lrig3*$^{-/-}$ mice (n=4 mice/genotype). C. Representative images of colonic cross sections comparing TUNEL identification of cell death between *Lrig3*$^{-/-}$ and WT mice. D. Scatterplot indicating significantly more cell death in the upper and lower portion of *Lrig3*$^{-/-}$ colonic crypts (n=6 mice/genotype). Significance was determined using an unpaired t-test, where significant difference between the groups is represented by an (*) when $p<0.05$ and (**) when $p<0.01$.

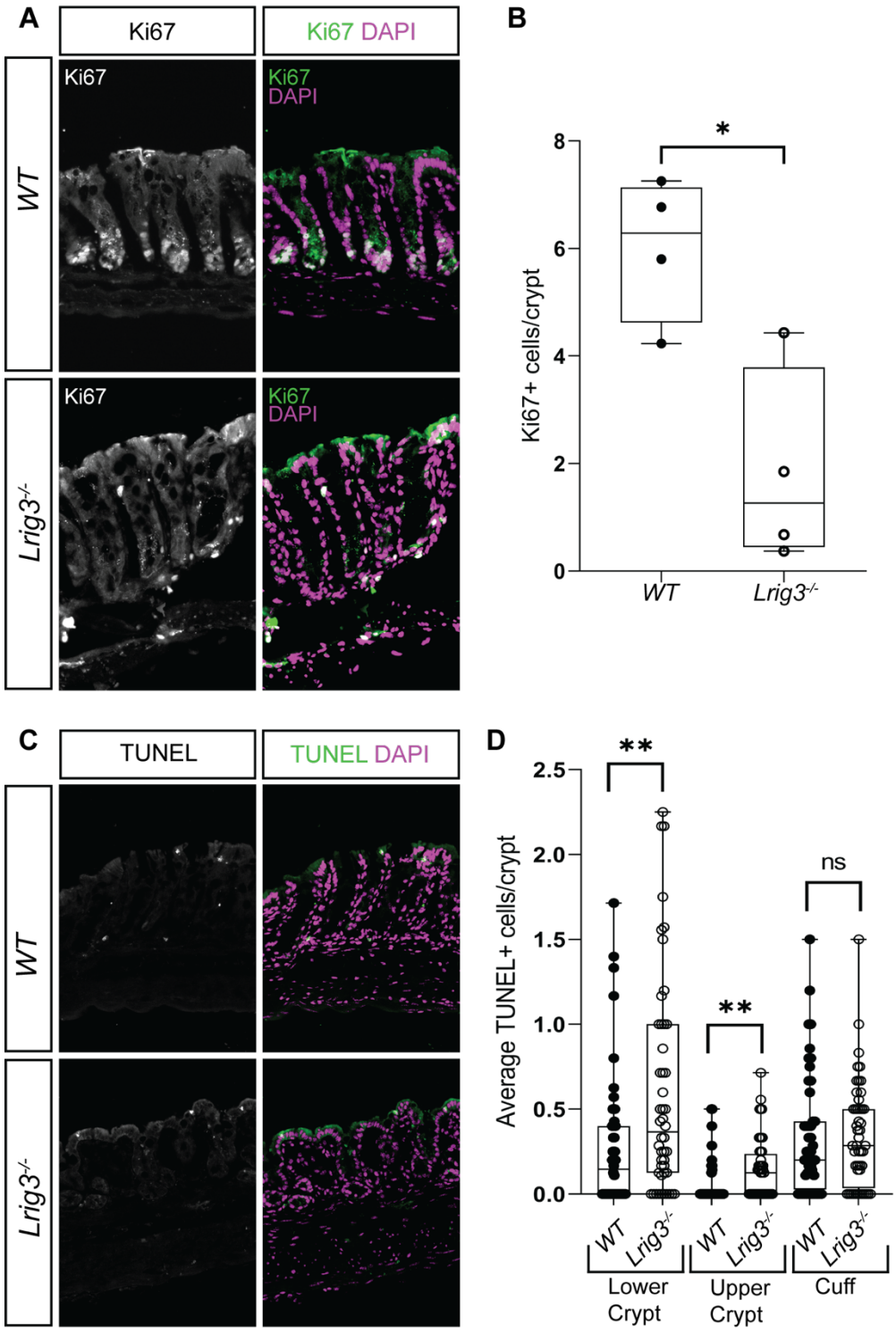

Figure 8. Cell proliferation decreases and cell death increases in Lrig3$^{-/-}$ mice following DSS

Together, our proliferation and cell death data in conjunction with the changes we observed in body weight lost, shortening of colon length, and decrease in crypt sizes support our hypothesis that Lrig3 is required for the protection against an inflammatory assault.

The loss of colonic epithelial cells caused by increased apoptosis, in the absence of Lrig3, is too high for the epithelium to fully regenerate and allow for recovery, even after the removal of DSS. This led us next to look for changes in the cellular composition of the *Lrig3*$^{-/-}$ mice to determine if changes in protein expression or cellular composition are also contributing to the inability of epithelial regeneration.

Stem Cells

To examine changes in the crypt-based stem cell compartment, we conducted immunofluorescent staining for the stem and progenitor cell marker, Lrig1 (Powell et al., 2012). In unpublished data from our lab, we have found that following DSS treatment, Lrig1 progressively increases expression above homeostatic levels at 24, 48, and 96 hours post DSS treatment Additionally, this same study found through single cell RNA sequencing of Lrig1+ cells, 48 hours after DSS treatment that WT mice have increased expression of Lrig3 transcripts (Jahahn et al., n.d.). This increase in both Lrig1 and Lrig3 following DSS treatment, combined with our previous data showing that *Lrig3*$^{-/-}$ mice have more Lrig1+ cells per colonic crypt than WT mice in homeostasis (Stevenson et al., 2022), led

us to hypothesize that there would be more Lrig1+ cells in the *Lrig3*$^{-/-}$ mice following DSS treatment.

We next used immunofluorescence imaging to examine changes to Lrig1 expression in the absence of Lrig3 compared to WT mice. *Lrig3*$^{-/-}$ crypts have fewer cells than WT crypts (Fig 6D), so we next asked what proportion of the colonic crypt contains Lrig1+ cells, compared to that of WT crypts. To quantify this data, we measured the total length of the crypt, from base to cuff, and then determined the length of the crypt which contained Lrig1+ cells. From this analysis we show that *Lrig3*$^{-/-}$ mice have proportionally fewer Lrig1+ cells per crypt than WT mice (Fig 9A-B). This is not the first time an increase in Lrig1 has been described, after changes in Lrig3, and this observation warrants further investigation. Nevertheless, as this data currently stands, our results indicate that Lrig3 is required for colon regeneration after inflammatory assault. In thinking about our results so far, I have several experimental avenues I would explore, if I were to continue this project. I will outline these thoughts for the rest of this chapter.

In the absence of Lrig3 expression during an inflammatory assault, and the resulting decrease in cell number, decreasing expression of Lrig1, we might expect to see an impact of the expression of a powerful growth modulator, Epidermal growth factor receptor. Based on the known regulation of Egfr by Lrig1 (Gur et al., 2004; Wong et al., 2012), we might expect to observe increased Egfr expression and consequently

increased proliferation, when Lrig1 is down regulated. We do not observe this increased proliferation, however, so future experiments exploring the growth signaling differences between WT and *Lrig3*$^{-/-}$ tissue will be critical. Clearly, our data indicate that WT animals can better protect the integrity of the colonic crypts during a DSS inflammatory assault, while also maintaining an appropriate proliferative response, compared to *Lrig3*$^{-/-}$ animals. WT animals increase Lrig1 expression, after inflammation, likely in order to regulate proliferation back to homeostatic levels; *Lrig3*$^{-/-}$ mice are missing this compensatory mechanism.

To investigate these observations further, I propose a set of future experiments. Going forward, I would perform two separate DSS time course studies. In the first, I would analyze protein and transcript expression patterns during each day of DSS treatment. This would create an expression 'timeline' of specific cellular markers both WT and *Lrig3*$^{-/-}$ mice, that would likely help us form hypotheses as to why the *Lrig3*$^{-/-}$ mice lack the ability to regenerate their colons. In the second, I would allow the *Lrig3*$^{-/-}$ mice that did not lose ~20% bodyweight to thrive for longer, thereby hopefully harnessing more data. Specifically, I would administer the 3% DSS for six days then switch the mice to plain water and allow the colonic epithelium to begin recovery. Although we previously ended the studies due to mice losing more than 20% of their starting body weight and overall, the *Lrig3*$^{-/-}$ mice lost a significantly larger percent of their body weight. Approximately 20% of the mice we

tested were under that threshold. For these, I would like to allow the mice to recover longer than 24 hours and create a timeline of specific stem cell markers and proliferation for the seven days following DSS treatment. These two studies will allow us to gain a clearer picture of changes to stemness markers, apoptosis, and proliferation changes in both WT and *Lrig3*$^{-/-}$ mice throughout DSS and during recovery.

As a final step in quantifying the cellular identify of cells present after DSS in both genotypes, we used Alcian blue to mark cells containing acidic epithelial mucins to identify any changes in the number of differentiated secretory cells of *Lrig3*$^{-/-}$ colonic crypts following DSS treatment. We quantified the proportion of the crypt that contained positively stained (blue) cells and binned them into four groups: 0-25%, 26-50%, 51-75%, and 76-100%. Through this preliminary analysis, we found that on average *Lrig3*$^{-/-}$ murine colonic crypts contain only a slightly higher proportion of mucus containing cells, but it is not significantly higher (Fig 9C-D; $p=0.19$). We currently have yet to identify any significant changes to differentiated cells within the *Lrig3*$^{-/-}$ colonic crypts following treatment with 3% DSS and 24 hours of recovery, suggesting that the loss of Lrig3 is more detrimental to regeneration of the stem cell compartment than to the differentiated secretory cells. Going forward, the next steps will be to identify changes in protein expression and cell signaling cascades within the *Lrig3*$^{-/-}$ colonic crypts. Determining changes in protein expression through immunofluorescence

analysis will allow us to recognize what cell types are present in the *Lrig3*$^{-/-}$ crypts and how it compares to the WT crypts following DSS treatment. Changes in cell signaling will be assayed through a phospho-Receptor Tyrosine Kinase (RTK) array to simultaneously identify changes in phosphorylation of 39 mouse specific RTK cell signaling proteins.

Conclusion

Our studies show *Lrig3*$^{-/-}$ mice undergo catastrophic crypt collapse, a shortened colon, and decreased body weight following DSS treatment (6 days of 3% DSS water and a 24-hour recovery on plain water) when compared to WT mice. At the crypt level of analysis, we see a significant decrease in total cell number per crypt, a significant decrease in proliferative cells, a significant decrease in the proportion of Lrig1+ cells, and a significant increase in apoptosis within the crypt. These results support the hypothesis that Lrig3 is required for regeneration in the colonic epithelium following an acute inflammatory injury, however, these results do not explain the role of Lrig3 in the regenerative process and additional information needs to be investigated in further studies.

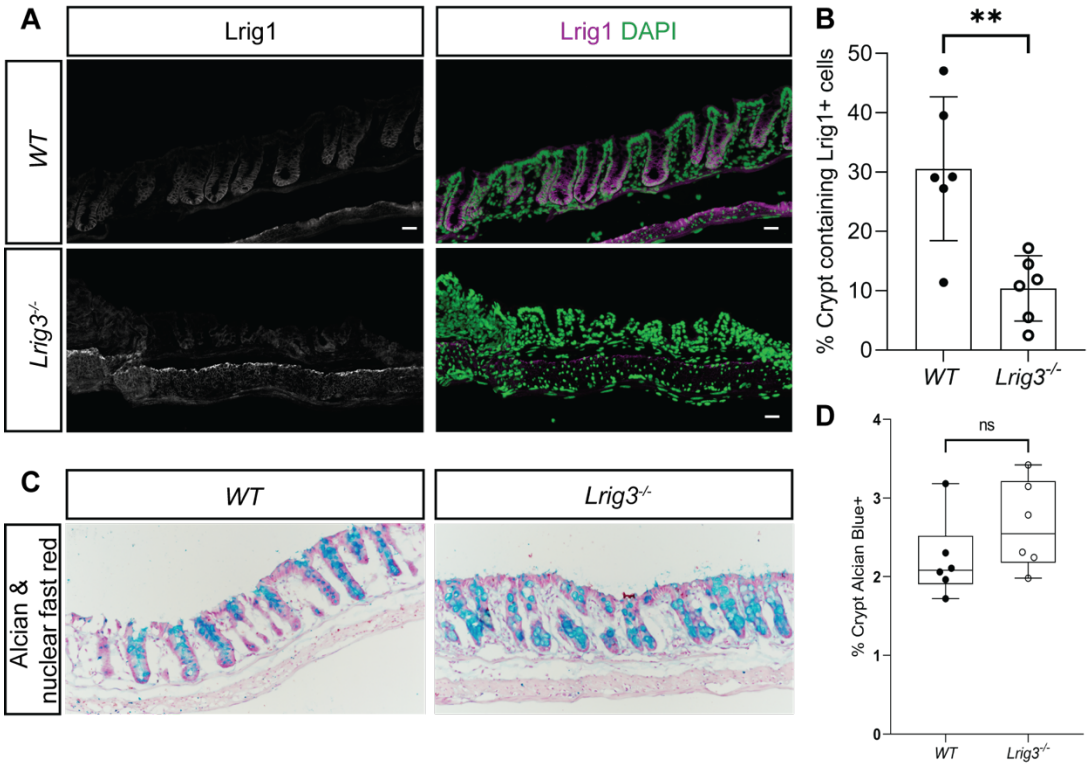

Figure 9. Expression of Lrig1 is decreased in Lrig3$^{-/-}$ mice following DSS *A. Representative images of colonic tissue sections comparing the expression of Lrig1 in* Lrig3$^{-/-}$ *and WT mice. B. Scatterplot indicating significantly less Lrig1+ cells in the Lrig3$^{-/-}$ crypts compared to WT (n=6 mice/genotype). C. Representative images of colonic tissue cross sections comparing alcian blue staining between* Lrig3$^{-/-}$ *and WT mice. D. Scatterplot indicating no significant change in alcian blue staining in the colonic crypts of* Lrig3$^{-/-}$ *and WT mice.*

Methods

Mice

C57BL/6 (WT) and *Lrig3$^{-/-}$* mice were housed in a specific pathogen-free environment under controlled light cycle conditions, fed standard rodent

lab chow, and provided water ad libitum. All mice were used at 6-10 weeks and mouse sex was mixed male to female at a roughly 50% ratio of each. All mice were sacrificed by cervical dislocation. At time of sacrifice, colons were removed, flushed with ice cold PBS and immediately measured using a ruler to obtain colon length, and then bifurcated. All procedures were approved and performed in accordance with the University of Oregon Institutional Animal Care and Use Committee.

DSS Treatment

Three percent dextran sodium sulfate (DSS) was dissolved in filtered drinking water and supplied ad libitum to WT and Lrig3 null mice for 6 days. Drinking water was switched to filtered water for 24 hours, then mice were sacrificed, and colons dissected for analysis. Mice are weighed daily to as an both an ethical precaution and a metric to track disease severity. If more than 20% of the mouse starting body weight is lost, the mice was sacrifice, per the ethical weight loss standards of the UO Institutional Animal Care and Use Committee (IACUC) standards. All procedures were approved and performed in accordance with the policies of the University of Oregon Institutional Animal Care and Use Committee.

Tissue Preparation for Staining

Tissue for paraffin and frozen block preparation were pinned onto a wax surface, fixed using 4% paraformaldehyde (PFA) for one hour, on a shaker at room temperature. They were then washed three times (five

minutes each) in PBS. For frozen blocks, tissue was submerged 30% sucrose in PBS overnight at 4°C and embedded in optimal tissue compound (OCT) for subsequent sectioning. For paraffin blocks, tissue was incubated in 70% ethanol and dehydrated in increasing alcohol baths and embedded in paraffin wax. All slides were sectioned at 7μm, (unless stated otherwise), and stained according to procedures below.

Antibodies and Staining Procedure

Frozen tissue slides were washed in PBS three times (three minutes each), blocked in 1% bovine serum albumin (BSA) and 0.03% Triton X-100 suspended in PBS for 1 hour. Antibodies were diluted in this blocking buffer at concentrations listed in Table 3, applied to the sections and sections were incubated overnight at 4°C. Slides were then washed in PBS three times (three minute each) and incubated with secondary antibodies at 1:500 in the same blocking buffer as above, for one hour at room temperature. Lastly, slides were washed in PBS for three minutes, then washed in PBS plus DAPI (1:10,000) for five minutes, and finally washed in PBS for three minutes. Slides were mounted using an n-propyl gallate/glycerol solution. Paraffin slides underwent conventional deparaffinization in xylenes and rehydration via ethanol washes and water, followed by antigen retrieval in a 1x Citrate buffer (ThermoFisher) in a pressure cooker for one hour. Antibody catalog information and concentrations used are listed in Table 3.

Table 3

Antibody	Company	Product#	Concentration
Lrig1	R&D Systems	AF3688	1:500 (IF)
Ki67(PE)	eBiosciences	SolA15	1:100 (IF)
Beta-catenin	Cell Signaling	19807	1:500

Image Acquisition and Analysis

Images for quantification of all immunofluorescent images were obtained using a Nikon Eclipse/Ds-Ri2 and NIS Elements software tools. Images were false-colored in Adobe Photoshop. All image analysis and quantifications were performed in a double-blind fashion and statistical comparisons were analyzed using GraphPad Prism software.

CHAPTER IV

CONCLUSIONS AND FUTURE DIRECTIONS

In this dissertation, I have presented a novel function for the transmembrane protein Lrig3 in the colonic epithelium. Prior to this body of work, Lrig3 had not been investigated in the colon. It was unknown what or if, Lrig3 had role in homeostasis or in regeneration. Through both the homeostasis (Chapter II) and regeneration (Chapter III) studies I show Lrig3 is required for cellular census of the stem cell compartment in homeostasis and is critical for epithelial regeneration in an IBD-like mouse model, respectively.

In Chapter II, the objective of my project was to define the influence of the loss of Lrig3 on colon biology. Using a novel mouse model with Lrig3 excised from the genome, I show through both transcript and protein expression analysis, that Lrig3 is expressed throughout the murine colonic crypt. I then describe, through histological and gross anatomy analysis, several morphological changes observed in the *Lrig3*$^{-/-}$ mice. These include shorter colons, larger mucosal area, and more cells per crypt. To investigate these alterations further, I show the *Lrig3*$^{-/-}$ crypts harbor a significant increase in the number and position of Lrig1^{+}, Lgr5^{+}, and Reg4^{+} cells. These data support a role for Lrig3 in the establishment of both colonic crypt structure and cellular census. To elucidate the molecular reasons for

these changes, we conducted immunofluorescent and western blot analysis to determine changes in receptor tyrosine kinase signaling pathways and found decreased activation of Erk (pErk). This observation suggests the perturbations we observe in the *Lrig3*$^{-/-}$ murine colonic epithelium may be occurring in an Erk-dependent manner. The continuance of this work is critical in understanding the relationship of Lrig3 and pErk in the colon and the disruptions of molecular mechanisms and signaling cascades that lead to the morphological and cellular census alterations we have identified.

In Chapter III, I demonstrate that *Lrig3*$^{-/-}$ mice undergo catastrophic crypt collapse, a shortened colon, and decreased body weight following an IBD-like regimen, when compared to WT mice. After analysis of the crypts, I show the *Lrig3*$^{-/-}$ mice have a significant decrease in the total number of cells and amount of proliferation per crypt, a significant decrease in the proportion of Lrig1+ cells, and a significant increase in apoptosis within the crypt. These results support the hypothesis that Lrig3 is required for regeneration in the colonic epithelium following an acute inflammatory injury, however, these results do not explain the molecular role for Lrig3 in the regenerative process. As the prevalence and disease burden of IBD increases annually it is imperative that regeneration in the colon is understood on a deeper level. Immunosuppressive therapies have long been the go-to for IBD treatment, but the long-term effects of chronic immune suppression

are known to have debilitating long-term side effects(Villablanca et al., 2022). Therefore, the future of IBD therapies ultimately depend on a greater understanding of the factors that influence proper colon regeneration after a bout of colitis.

The work I have completed in my dissertation clearly show the requirement of Lrig3 in regeneration; however, we have not revealed how Lrig3 is regulating regeneration in the wildtype animals. Determining how Lrig3 may be functionally regulating proper Lrig1 expression, proliferation, apoptosis, and therefore appropriate cellular census of the colonic crypt are necessary. To continue answering this question the next set of experiments will focus on finding changes in cell signaling cascades within the *Lrig3*$^{-/-}$ colonic epithelium, specifically receptor tyrosine kinases such as Erk and Egfr that regulate many pathways involved in stem cell renewal, cell proliferation, differentiation, and migration in mammals and within the colon(Brandt et al., 2019; Lu et al., 2014; Procaccino et al., 1994; Zeng et al., 2020b).

As discussed in Chapter III, future studies investigating the role of Lrig3 in regeneration after an IBD-like state, include additional time course studies. Going forward, it will be important to perform DSS treatments, and quantify expression of key proteins each day of the six-day time course, and of DSS each day of recovery (reversion to water) for up to 14 days, or until each *Lrig3*$^{-/-}$ mouse must be removed from the study due to excessive weight loss. These studies will likely give us a

better understanding of the fluctuations in relevant cell signaling cascades impacted by the loss of Lrig3. For the mice that must be sacrificed due to >20% weight loss before reaching 14 days of recovery, this will also allow us to examine molecular and cellular differences in a spatial and temporal model that is at the peak of catastrophic failure.

One aspect of the role of Lrig3 in colon biology that remains unexplored in my dissertation is the role of Lrig3 in murine colon development. At six-to-ten weeks of age, unperturbed *Lrig3*$^{-/-}$ mice have an expanded stem cell compartment and larger mucosal area. This suggests that not only does Lrig3 have a role in stem cell compartment census, but that there may also be developmental defects in the morphogenesis of the colon. The current scientific literature on the development of the colon is very limited (Ménard et al., 1994; Noah et al., 2011; Wei et al., 2020), and this mouse model has the potential to greatly contribute to the open question of how colonic crypts develop and the epithelium is established.

In closing, for my doctoral dissertation, I set out to identify the molecular mechanisms of that govern colon crypt homeostasis and regeneration. By utilizing a novel *Lrig3*$^{-/-}$ mouse model, I ultimately was able to address several open questions regarding the regulation of crypt cellular census and identify a critical protein in epithelial regeneration. Although my work has focused on the role of Lrig3 in the murine colon, it contributes to a more complete understanding of how the colon regulates

the continual renewal and regeneration of the epithelial barrier, for the entire life of an organism. And, though the complete molecular mechanisms remain to be determined, this body of work supports the necessity to continue researching Lrig3 in the colon and truly understand colonic development, homeostasis, and regeneration from injury.

APPENDICES

A. Supplemental Figure 1

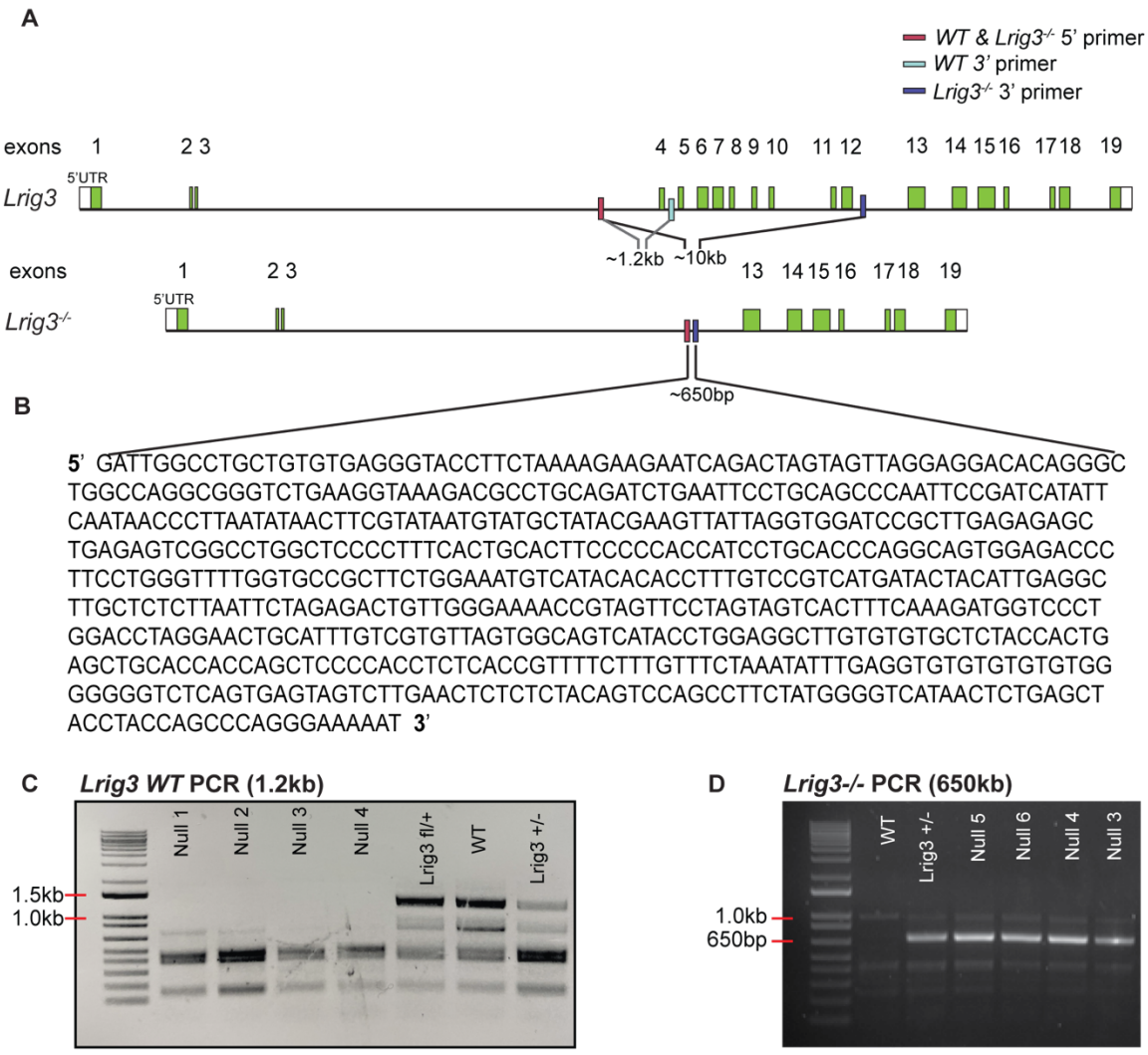

Supplemental Figure 1. Wildtype and *Lrig3*$^{-/-}$ allele map, sequence, and PCR screening of mice. A-B. Schematic representation of the wildtype and *Lrig3*$^{-/-}$ genes. Disruption of Lrig3 was achieved through the removal of exons 4-12, joining the third and twelfth intron. B. The intervening remaining sequence (650bp) is shown. C. Confirmatory PCR analysis of the wildtype Lrig3 allele, using primers that are located upstream (5') and downstream (3') of the fourth exon, and generate 1.2kb PCR product. *Lrig3*$^{-/-}$ mice do not generate a PCR product, as they lack the 3' site. D. Confirmatory PCR analysis of the null Lrig3 allele, using primers that are located upstream (5') of the fourth exon and downstream (3') of the twelfth

exon, generates a 650bp product in the null mice. Wildtype mice do not generate a PCR product under standard conditions, as that region is 10kb in length. Lrig3 mutant heterozygous and homozygous mice are viable and fertile. PCR primer sequences are listed in Supplemental Table 1.

B. Supplemental Figure 2

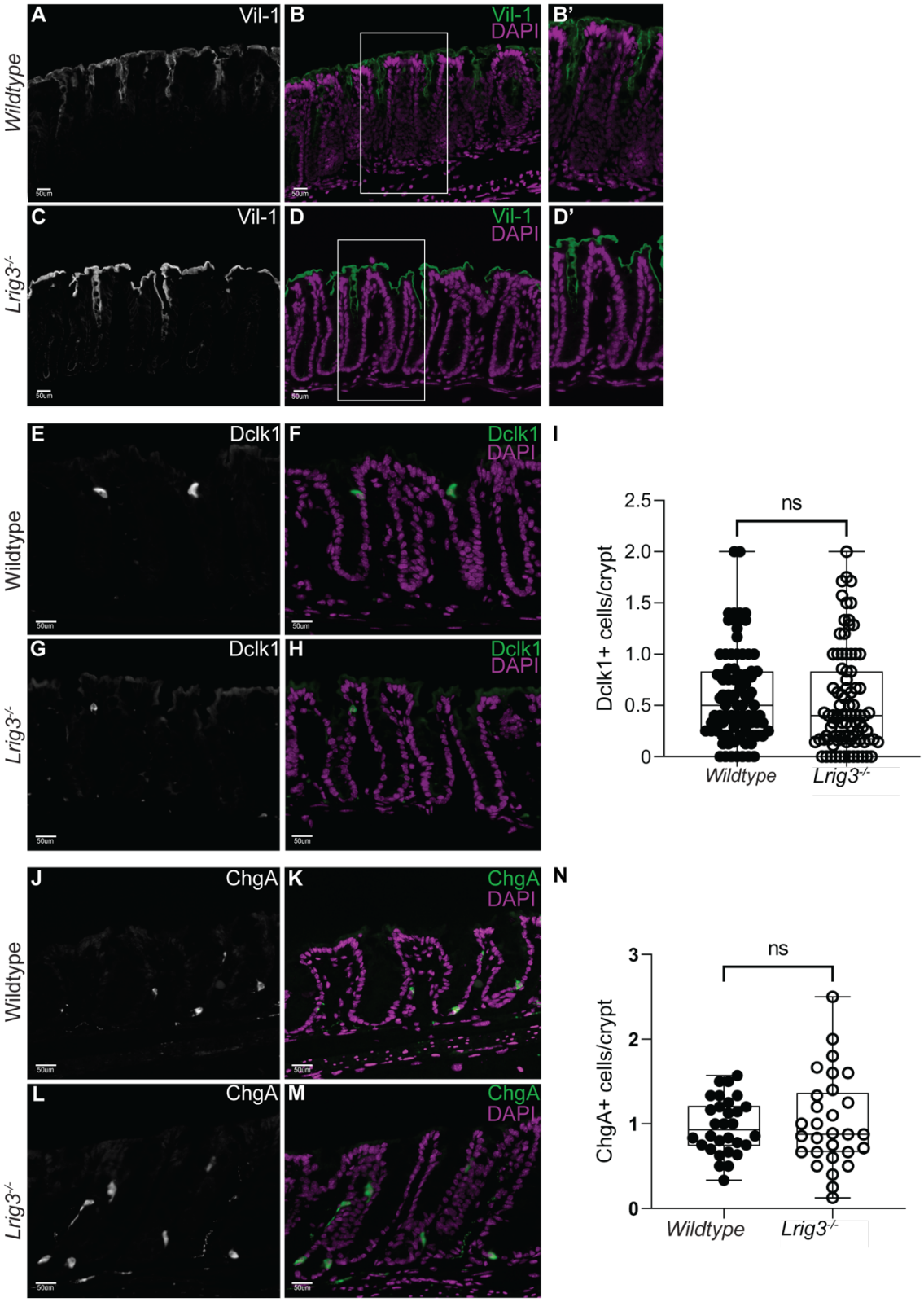

Supplemental Figure 2. Differentiated Cell marker expression in *Lrig3*$^{-/-}$ and wildtype colons. A-D. Representative images of Vil-1 expression (green) in the absorptive cells of the colonic epithelium in wildtype (A-B) *Lrig3*$^{-/-}$ colons (C-D). B' and D'. Enlarged images of Vil-1 expression shown in wildtype (B and B') and *Lrig3*$^{-/-}$ (D and D'). E-H. Representative images of Dclk1 expression (green) in tuft cells of colonic epithelium in wildtype (E-F) *Lrig3*$^{-/-}$ (G-H) colons. I. Scatter plot indicating no significant change in Dclk1^{+} cells in the colonic crypts of *Lrig3*$^{-/-}$ compared to wildtype mice (n=4, 10 images/mouse). J-M. representative images of ChgA expression (green) in neuroendocrine cells of the colonic epithelium in wildtype (J-K) and *Lrig3*$^{-/-}$ (L-M) colons. N. Scatter plot indicating no significant change in ChgA^{+} cells in the colonic epithelium of *Lrig3*$^{-/-}$ compared to wildtype mice (n=4, 10 images/mouse). For both panels, nuclei in are depicted in magenta and the scale bar indicates 50um.

REFERENCES CITED

Abousoliman, I., Reyer, H., Oster, M., Murani, E., Mohamed, I., & Wimmers, K. (2021). Genome-Wide Analysis for Early Growth-Related Traits of the Locally Adapted Egyptian Barki Sheep. *Genes*, *12*(8). https://doi.org/10.3390/genes12081243

Abraira, V. E., del Rio, T., Tucker, A. F., Slonimsky, J., Keirnes, H. L., & Goodrich, L. v. (2008). Cross-repressive interactions between Lrig3 and netrin 1 shape the architecture of the inner car. *Development*, *135*(24). https://doi.org/10.1242/dev.029330

Abraira, V. E., Satoh, T., Fekete, D. M., & Goodrich, L. v. (2010). Vertebrate Lrig3-ErbB interactions occur in vitrobut are unlikely to play a role in Lrig3-dependent inner ear morphogenesis. *PLoS ONE*, *5*(2). https://doi.org/10.1371/journal.pone.0008981

Alatab, S., Sepanlou, S. G., Ikuta, K., Vahedi, H., Bisignano, C., Safiri, S., Sadeghi, A., Nixon, M. R., Abdoli, A., Abolhassani, H., Alipour, V., Almadi, M. A. H., Almasi-Hashiani, A., Anushiravani, A., Arabloo, J., Atique, S., Awasthi, A., Badawi, A., Baig, A. A. A., … Naghavi, M. (2020). The global, regional, and national burden of inflammatory bowel disease in 195 countries and territories, 1990–2017: a systematic analysis for the Global Burden of Disease Study 2017. *The Lancet Gastroenterology & Hepatology*, *5*(1), 17–30. https://doi.org/10.1016/S2468-1253(19)30333-4

Araki, Y., Mukaisyo, K.-I., Sugihara, H., Fujiyama, Y., & Hattori, T. (2010). Increased apoptosis and decreased proliferation of colonic epithelium in dextran sulfate sodium-induced colitis in mice. *Oncology Reports*, *24*(4), 869–874.

B. Egger J. Lakshmanan, P. Moore, V. E. Eysselein, M. W. B. (2000). Mice Harboring a Defective Epidermal Growth Factor Receptor-(Waved-2) Have an Increased Susceptibility to Acute Dextran-Sulfate-induced Colitis. *Scandinavian Journal of Gastroenterology*, *35*(11), 1181–1187. https://doi.org/10.1080/003655200750056664

Barker, N. (2013). Adult intestinal stem cells: critical drivers of epithelial homeostasis and regeneration. *Nature Reviews Molecular Cell Biology*, *15*, 19. http://dx.doi.org/10.1038/nrm3721

Barker, N., van Es, J. H., Kuipers, J., Kujala, P., van den Born, M., Cozijnsen, M., Haegebarth, A., Korving, J., Begthel, H., Peters, P. J., & Clevers, H. (2007). Identification of stem cells in small intestine and colon by marker gene Lgr5. *Nature*, *449*, 1003. http://dx.doi.org/10.1038/nature06196

Brandt, R., Sell, T., Lüthen, M., Uhlitz, F., Klinger, B., Riemer, P., Giesecke-Thiel, C., Schulze, S., El-Shimy, I. A., Kunkel, D., Fauler, B., Mielke, T., Mages, N., Herrmann, B. G., Sers, C., Blüthgen, N., & Morkel, M. (2019). Cell type-dependent differential activation of ERK by oncogenic KRAS in colon cancer and intestinal epithelium. *Nature Communications*, *10*(1), 2919. https://doi.org/10.1038/s41467-019-10954-y

Brown, D. C., & Gatter, K. C. (2002). Ki67 protein: the immaculate deception? *Histopathology*, *40*(1), 2–11. https://doi.org/https://doi.org/10.1046/j.1365-2559.2002.01343.x

Cai, M., Xie, R., Han, L., Chen, R., Wang, B., Ye, F., Guo, D., & Lei, T. (2009). Effects of RNAi-mediated gene silencing of LRIG3 expression on cell cycle and survival of glioma cells. *Journal of Huazhong University of Science and Technology - Medical Science*, *29*(1). https://doi.org/10.1007/s11596-009-0119-z

Castillo-Azofeifa, D., Fazio, E. N., Nattiv, R., Good, H. J., Wald, T., Pest, M. A., de Sauvage, F. J., Klein, O. D., & Asfaha, S. (2019). Atoh1(+) secretory progenitors possess renewal capacity independent of Lgr5(+) cells during colonic regeneration. *The EMBO Journal*, e99984. https://doi.org/10.15252/embj.201899984

Chassaing, B., Aitken, J. D., Malleshappa, M., & Vijay-Kumar, M. (2014). Dextran Sulfate Sodium (DSS)-Induced Colitis in Mice. *Current Protocols in Immunology / Edited by John E. Coligan ... [et Al.]*, *104*, Unit-15.25. https://doi.org/10.1002/0471142735.im1525s104

Chen, Y., Wang, Q., Wang, M., & Li, M. (2019). Overexpressed LRIG3 gene ameliorates prostate cancer through suppression of cell invasion and migration. *International Journal of Biological Macromolecules*, *124*, 1–9. https://doi.org/https://doi.org/10.1016/j.ijbiomac.2018.11.028

Cochran, K. E., Lamson, N. G., & Whitehead, K. A. (2020). Expanding the utility of the dextran sulfate sodium (DSS) mouse model to induce a clinically relevant loss of intestinal barrier function. *PeerJ*, *8*, e8681–e8681. https://doi.org/10.7717/peerj.8681

Dahlhamer, J. M., Zammitti, E. P., Ward, B. W., Wheaton, A. G., & Croft, J. B. (2016). Prevalence of Inflammatory Bowel Disease Among Adults Aged ≥18 Years — United States, 2015. *MMWR. Morbidity and Mortality Weekly Report*, *65*(42), 1166–1169. https://doi.org/10.15585/mmwr.mm6542a3

de Vincenti, A. P., Alsina, F. C., Ferrero Restelli, F., Hedman, H., Ledda, F., & Paratcha, G. (2021). Lrig1 and Lrig3 cooperate to control Ret receptor signaling, sensory axonal growth and epidermal innervation. *Development*, *148*(16). https://doi.org/10.1242/dev.197020

del Rio, T., Nishitani, A. M., Yu, W.-M., & Goodrich, L. v. (2013). In Vivo Analysis of Lrig Genes Reveals Redundant and Independent Functions in the Inner Ear. *PLOS Genetics*, *9*(9), e1003824. https://doi.org/10.1371/journal.pgen.1003824

Dessimoz, J., Opoka, R., Kordich, J. J., Grapin-Botton, A., & Wells, J. M. (2006). FGF signaling is necessary for establishing gut tube domains alongthe anterior–posterior axis in vivo. *Mechanisms of Development*, *123*(1), 42–55. https://doi.org/https://doi.org/10.1016/j.mod.2005.10.001

Eichele, D. D., & Kharbanda, K. K. (2017). Dextran sodium sulfate colitis murine model: An indispensable tool for advancing our understanding of inflammatory bowel diseases pathogenesis. *World Journal of Gastroenterology*, *23*(33), 6016–6029. https://doi.org/10.3748/wjg.v23.i33.6016

Fendrik, A. J., Romanelli, L., & Rotondo, E. (2018). Neutral dynamics and cell renewal of colonic crypts in homeostatic regime. *Physical Biology*, *15*(3), 036003. https://doi.org/10.1088/1478-3975/aaab9f

Gehart, H., & Clevers, H. (2019). Tales from the crypt: new insights into intestinal stem cells. *Nature Reviews Gastroenterology & Hepatology*, *16*(1), 19–34. https://doi.org/10.1038/s41575-018-0081-y

Genepaint. (n.d.). https://gp3.mpg.de

Girish, N., Liu, C. Y., Gadeock, S., Gomez, M. L., Huang, Y., Sharifkhodaei, Z., Washington, M. K., & Polk, D. B. (2021). Persistence of Lgr5+ colonic epithelial stem cells in mouse models of inflammatory bowel disease. *American Journal of Physiology-Gastrointestinal and Liver Physiology*, *321*(3), G308–G324. https://doi.org/10.1152/ajpgi.00248.2020

Gur, G., Rubin, C., Katz, M., Amit, I., Citri, A., Nilsson, J., Amariglio, N., Henriksson, R., Rechavi, G., Hedman, H., Wides, R., & Yarden, Y. (2004). LRIG1 restricts growth factor signaling by enhancing receptor ubiquitylation and degradation. *The EMBO Journal*, *23*(16), 3270–3281. https://doi.org/10.1038/sj.emboj.7600342

Hellström, M., Ericsson, M., Johansson, B., Faraz, M., Anderson, F., Henriksson, R., Nilsson, S. K., & Hedman, H. (2016). Cardiac hypertrophy and decreased high-density lipoprotein cholesterol in Lrig3-deficient mice. *American Journal of Physiology - Regulatory, Integrative and Comparative Physiology*, *310*(11), R1045. http://ajpregu.physiology.org/content/310/11/R1045.abstract

Henning, S. J., & von Furstenberg, R. J. (2016). GI stem cells – new insights into roles in physiology and pathophysiology. *The Journal of Physiology*, *594*(17), 4769–4779. https://doi.org/https://doi.org/10.1113/JP271663

Hu, X., Zhou, K., Cao, S., Zhu, H., & Xie, K. (2021). Circ_lrig3 contributes to the progression of hepatocellular carcinoma by elevating rnf38 via sponging mir-449a. *General Physiology and Biophysics*, *40*(2). https://doi.org/10.4149/gpb_2020044

Jahahn, N. J., Mohr, B. M., Lantz, T. L., Pellitier, N., & Zemper, A. E. (n.d.). Lrig1-based lineage tracing has distinct patterns within the context of DSS colitis recovery. *Unpublished*.

Kiesler, P., Fuss, I. J., & Strober, W. (2015). Experimental Models of Inflammatory Bowel Diseases. *Cellular and Molecular Gastroenterology and Hepatology*, *1*(2), 154–170. https://doi.org/10.1016/j.jcmgh.2015.01.006

Kwon, O., Han, T.-S., & Son, M.-Y. (2020). Intestinal Morphogenesis in Development, Regeneration, and Disease: The Potential Utility of Intestinal Organoids for Studying Compartmentalization of the Crypt-Villus Structure. *Frontiers in Cell and Developmental Biology*, *8*, 593969. https://doi.org/10.3389/fcell.2020.593969

Liu, P., Jenkins, N. A., & Copeland, N. G. (2003). A highly efficient recombineering-based method for generating conditional knockout mutations. *Genome Research*, *13*(3), 476–484. https://doi.org/10.1101/gr.749203

Lu, N., Wang, L., Cao, H., Liu, L., van Kaer, L., Washington, M. K., Rosen, M. J., Dube, P. E., Wilson, K. T., Ren, X., Hao, X., Polk, D. B., & Yan, F. (2014). Activation of the epidermal growth factor receptor in macrophages regulates cytokine production and experimental colitis. *Journal of Immunology (Baltimore, Md. : 1950)*, *192*(3), 1013–1023. https://doi.org/10.4049/jimmunol.1300133

Lucafò, M., Curci, D., Franzin, M., Decorti, G., & Stocco, G. (2021). Inflammatory Bowel Disease and Risk of Colorectal Cancer: An Overview From Pathophysiology to Pharmacological Prevention. *Frontiers in Pharmacology*, *12*. https://www.frontiersin.org/article/10.3389/fphar.2021.772101

Ménard, D., Dagenais, P., & Calvert, R. (1994). Morphological changes and cellular proliferation in mouse colon during fetal and postnatal development. *The Anatomical Record*, *238*(3), 349–359. https://doi.org/10.1002/ar.1092380309

Metodiev, S., Thekkoot, D. M., Young, J. M., Onteru, S., Rothschild, M. F., & Dekkers, J. C. M. (2018). A whole-genome association study for litter size and litter weight traits in pigs. *Livestock Science*, *211*. https://doi.org/10.1016/j.livsci.2018.03.004

Murata, K., Jadhav, U., Madha, S., van Es, J., Dean, J., Cavazza, A., Wucherpfennig, K., Michor, F., Clevers, H., & Shivdasani, R. A. (2020). Ascl2-Dependent Cell Dedifferentiation Drives Regeneration of Ablated Intestinal Stem Cells. *Cell Stem Cell*, *26*(3), 377-390.e6. https://doi.org/https://doi.org/10.1016/j.stem.2019.12.011

Noah, T. K., Donahue, B., & Shroyer, N. F. (2011). Intestinal development and differentiation. *Experimental Cell Research*, *317*(19), 2702–2710. https://doi.org/10.1016/j.yexcr.2011.09.006

Osaki, L. H., & Gama, P. (2013). MAPKs and Signal Transduction in the Control of Gastrointestinal Epithelial Cell Proliferation and Differentiation. *International Journal of Molecular Sciences*, *14*(5), 10143–10161. https://doi.org/10.3390/ijms140510143

Park, K. T., Ehrlich, O. G., Allen, J. I., Meadows, P., Szigethy, E. M., Henrichsen, K., Kim, S. C., Lawton, R. C., Murphy, S. M., Regueiro, M., Rubin, D. T., Engel-Nitz, N. M., & Heller, C. A. (2020). The Cost of Inflammatory Bowel Disease: An Initiative From the Crohn's & Colitis Foundation. *Inflammatory Bowel Diseases*, *26*(1), 1–10. https://doi.org/10.1093/ibd/izz104

Peng, C., Chen, H., Li, Y., Yang, H., Qin, P., Ma, B., Duan, Q., Wang, B., Mao, F., & Guo, D. (2021). LRIG3 Suppresses Angiogenesis by Regulating the PI3K/AKT/VEGFA Signaling Pathway in Glioma. *Frontiers in Oncology*, *11*, 54. https://doi.org/10.3389/fonc.2021.621154

Peng, J., Han, S., Chen, Z., Yang, J., Pei, Y., Bao, C., Qiao, L., Chen, W., & Liu, B. (2020). Chaperone-mediated autophagy regulates apoptosis and the proliferation of colon carcinoma cells. *Biochemical and Biophysical Research Communications*, *522*(2), 348–354. https://doi.org/https://doi.org/10.1016/j.bbrc.2019.11.081

Powell, A. E., Wang, Y., Li, Y., Poulin, E. J., Means, A. L., Washington, M. K., Higginbotham, J. N., Juchheim, A., Prasad, N., Levy, S. E., Guo, Y., Shyr, Y., Aronow, B. J., Haigis, K. M., Franklin, J. L., & Coffey, R. J. (2012). The pan-ErbB negative regulator, Lrig1, is an intestinal stem cell marker that functions as a tumor suppressor. *Cell*, *149*(1), 146–158. https://doi.org/10.1016/j.cell.2012.02.042

Procaccino, F., Reinshagen, M., Hoffmann, P., Zeeh, J. M., Lakshmanan, J., McRoberts, J. A., Patel, A., French, S., & Eysselein, V. E. (1994). Protective effect of epidermal growth factor in an experimental model of colitis in rats. *Gastroenterology*, *107*(1), 12–17. https://doi.org/https://doi.org/10.1016/0016-5085(94)90055-8

Qiu, Y., Han, Q., Lu, H., & Shi, C. (2020). miR-196a targeting LRIG3 promotes the proliferation and migration of cervical cancer cells. *Cellular and Molecular Biology*, *66*(7). https://doi.org/10.14715/cmb/2020.66.7.27

Ramachandran, A., Madesh, M., & Balasubramanian, K. A. (2000). Apoptosis in the intestinal epithelium: Its relevance in normal and pathophysiological conditions. *Journal of Gastroenterology and Hepatology*, *15*(2), 109–120. https://doi.org/https://doi.org/10.1046/j.1440-1746.2000.02059.x

Sasaki, N., Sachs, N., Wiebrands, K., Ellenbroek, S. I. J., Fumagalli, A., Lyubimova, A., Begthel, H., van Born, M. den, van Es, J. H., Karthaus, W. R., Li, V. S. W., López-Iglesias, C., Peters, P. J., van Rheenen, J., van Oudenaarden, A., & Clevers, H. (2016). Reg4+ deep crypt secretory cells function as epithelial niche for Lgr5+ stem cells in colon. *Proceedings of the National Academy of Sciences of the United States of America*, *113*(37), E5399–E5407. https://doi.org/10.1073/pnas.1607327113

Schlieve, C. R., Mojica, S. G., Holoyda, K. A., Hou, X., Fowler, K. L., & Grikscheit, T. C. (2016). Vascular Endothelial Growth Factor (VEGF) Bioavailability Regulates Angiogenesis and Intestinal Stem and Progenitor Cell Proliferation during Postnatal Small Intestinal Development. *PLOS ONE*, *11*(3), e0151396. https://doi.org/10.1371/journal.pone.0151396

Simion, C., Prieto, M. E. C., & Sweeney, C. (2014). The LRIG family – enigmatic regulators of growth factor receptor signaling. *Endocrine-Related Cancer*, *21*(6), R431–R443. https://doi.org/10.1530/ERC-14-0179

Stevenson, J. G., Sayegh, R., Pedicino, N., Pellitier, N. A., Wheeler, T., Bechard, M. E., Huh, W. J., Coffey, R. J., & Zemper, A. E. (2022). lrig3-restricts-the-size-of-the-colon-stem-cell-compartment. *American Journal of Physiology - Gastrointestinal and Liver Physiology*.

Sun, H., Zhai, J., Zhang, L., & Chen, Y. (2021). CircRNA LRIG3 knockdown inhibits hepatocellular carcinoma progression by regulating miR-223-3p and MAPK/ERK pathway. *Archives of Medical Science*. https://doi.org/10.5114/aoms/124975

Sun, S., Gao, J., Zhou, S., Li, Y., Wang, Y., Jin, L., Li, J., Liu, B., Zhang, B., Han, S., Ding, H., & Li, X. (2020). A novel circular RNA circ-LRIG3 facilitates the malignant progression of hepatocellular carcinoma by modulating the EZH2/STAT3 signaling. *Journal of Experimental & Clinical Cancer Research*, *39*(1), 252. https://doi.org/10.1186/s13046-020-01779-5

Tikhonova, A. N., Lasry, A., Austin, R., & Aifantis, I. (2020). Cell-by-Cell Deconstruction of Stem Cell Niches. *Cell Stem Cell*, *27*(1), 19–34. https://doi.org/10.1016/J.STEM.2020.06.013

Tóth, B., Ben-Moshe, S., Gavish, A., Barkai, N., & Itzkovitz, S. (2017). Early commitment and robust differentiation in colonic crypts. *Molecular Systems Biology*, *13*(1), 902. https://doi.org/https://doi.org/10.15252/msb.20167283

van der Flier, L. G., & Clevers, H. (2009). Stem Cells, Self-Renewal, and Differentiation in the Intestinal Epithelium. *Annual Review of Physiology*, *71*(1), 241–260. https://doi.org/10.1146/annurev.physiol.010908.163145

Villablanca, E. J., Selin, K., & Hedin, C. R. H. (2022). Mechanisms of mucosal healing: treating inflammatory bowel disease without immunosuppression? *Nature Reviews Gastroenterology & Hepatology*. https://doi.org/10.1038/s41575-022-00604-y

Wang, Y., Shi, C., Lu, Y., Poulin, E. J., Franklin, J. L., & Coffey, R. J. (2015). Loss of Lrig1 leads to expansion of Brunner glands followed by duodenal adenomas with gastric metaplasia. *The American Journal of Pathology*, *185*(4), 1123–1134. https://doi.org/10.1016/j.ajpath.2014.12.014

Wei, G., Gao, N., Chen, J., Fan, L., Zeng, Z., Gao, G., Li, L., Fang, G., Hu, K., Pang, X., Fan, H.-Y., Clevers, H., Liu, M., Zhang, X., & Li, D. (2020). ERK/MAPK signaling is essential for intestinal development through Wnt pathway modulation. *Development*, dev.185678. https://doi.org/10.1242/dev.185678

Wong, V. W. Y., Stange, D. E., Page, M. E., Buczacki, S., Wabik, A., Itami, S., van de Wetering, M., Poulsom, R., Wright, N. A., Trotter, M. W. B., Watt, F. M., Winton, D. J., Clevers, H., & Jensen, K. B. (2012). Lrig1 controls intestinal stem cell homeostasis by negative regulation of ErbB signalling. *Nature Cell Biology*, *14*(4), 401–408. https://doi.org/10.1038/ncb2464

Xavier, R. J., & Podolsky, D. K. (2007). Unravelling the pathogenesis of inflammatory bowel disease. *Nature*, *448*(7152), 427–434. https://doi.org/10.1038/nature06005

Yeshi, K., Ruscher, R., Hunter, L., Daly, N. L., Loukas, A., & Wangchuk, P. (2020). Revisiting Inflammatory Bowel Disease: Pathology, Treatments, Challenges and Emerging Therapeutics Including Drug Leads from Natural Products. *Journal of Clinical Medicine*, *9*(5), 1273. https://doi.org/10.3390/jcm9051273

Yui, S., Azzolin, L., Maimets, M., Pedersen, M. T., Fordham, R. P., Hansen, S. L., Larsen, H. L., Guiu, J., Alves, M. R. P., Rundsten, C. F., Johansen, J. v, Li, Y., Madsen, C. D., Nakamura, T., Watanabe, M., Nielsen, O. H., Schweiger, P. J., Piccolo, S., & Jensen, K. B. (2018). YAP/TAZ-Dependent Reprogramming of Colonic Epithelium Links ECM Remodeling to Tissue Regeneration. *Cell Stem Cell*, *22*(1), 35-49.e7. https://doi.org/10.1016/j.stem.2017.11.001

Zeng, K., Chen, X., Xu, M., Liu, X., Li, C., Xu, X., Pan, B., Qin, J., He, B., Pan, Y., Huiling, S., Xu, T., & Wang, S. (2020a). LRIG3 represses cell motility by inhibiting slug via inactivating ERK signaling in human colorectal cancer. *IUBMB Life*, *December 2019*, 1–11. https://doi.org/10.1002/iub.2262

Zeng, K., Chen, X., Xu, M., Liu, X., Li, C., Xu, X., Pan, B., Qin, J., He, B., Pan, Y., Huiling, S., Xu, T., & Wang, S. (2020b). LRIG3 represses cell motility by inhibiting slug via inactivating ERK signaling in human colorectal cancer. *IUBMB Life*, *December 2019*, 1–11. https://doi.org/10.1002/iub.2262

Zhang, Y.-Z., & Li, Y.-Y. (2014). Inflammatory bowel disease: pathogenesis. *World Journal of Gastroenterology*, *20*(1), 91–99. https://doi.org/10.3748/wjg.v20.i1.91

Zhao, H., Tanegashima, K., Ro, H., & Dawid, I. B. (2008). Lrig3 regulates neural crest formation in Xenopus by modulating Fgf and Wnt signaling pathways. *Development (Cambridge, England)*, *135*(7), 1283–1293. https://doi.org/10.1242/dev.015073

Zhou, H., Cao, J., Yang, F., Fan, D., Li, H., Fan, T., & Sun, P. (2021). Member Domain 3 (LRIG3) Activates Hypoxia-Inducible Factor-1 α /Vascular Endothelial Growth Factor (HIF-1 α /VEGF) Pathway to Inhibit the Growth of Bone Marrow Mesenchymal Stem Cells in Glioma . *Journal of Biomaterials and Tissue Engineering*, *11*(5). https://doi.org/10.1166/jbt.2021.2629